เส้นใยจากพอลิเมอร์คอมพอสิตของพอลิสไตรีนและพอลิฮีดรัลโอลิโกเมอริกซิลเซสควิออกเซน

นายธนรัตน์ ภิสัชเพ็ญ

วิทยานิพนธ์นี้เป็นส่วนหนึ่งของการศึกษาตามหลักสูตรปริญญาวิทยาศาสตรมหาบัณฑิต
สาขาวิชาเคมี ภาควิชาเคมี
คณะวิทยาศาสตร์ จุฬาลงกรณ์มหาวิทยาลัย
ปีการศึกษา 2554

FIBER FROM POLYMER COMPOSITE OF POLYSTYRENE AND POLYHEDRAL
OLIGOMERIC SILSESQUIOXANE

Mr. Thanarath Pisuchpen

A Thesis Submitted in Partial Fulfillment of the Requirements
for the Degree of Master of Science Program in Chemistry
Department of Chemistry
Faculty of Science
Chulalongkorn University
Academic Year 2011

Thesis Title   FIBER FROM POLYMER COMPOSITE OF POLYSTYRENE AND POLYHEDRAL OLIGOMERIC SILSESQUIOXANE

By   Mr. Thanarath Pisuchpen

Field of Study   Chemistry

Thesis Advisor   Associate Professor Voravee P. Hoven, Ph.D.

Thesis Co-advisor   Varol Intasanta, Ph.D.

Accepted by the Faculty of Science, Chulalongkorn University in Partial Fulfillment of the Requirements for the Master's Degree

…………………………………..……….Dean of the Faculty of Science

(Professor Supot Hannongbua, Dr.rer.nat.)

THESIS COMMITEE

…………………………………………….Chairman

(Assistant Professor Aroonsiri Shitangkoon, Ph.D.)

…………………………………………….Thesis Advisor

(Associate Professor Voravee P. Hoven, Ph.D.)

…………………………………………….Thesis Co-advisor

(Varol Intasanta, Ph.D.)

…………………………………………….Examiner

(Associate Professor Nuanphun Chantarasiri, Ph.D.)

…………………………………………….External Examiner

(Gamolwan Tumcharern, Ph.D.)

ธนรัตน์ ภิสัชเพ็ญ: เส้นใยจากพอลิเมอร์คอมพอสิตของพอลิสไตรีนและพอลิฮีดรัลโอลิโกเมอริกซิลเสสควิออกเซน. (FIBER FROM POLYMER COMPOSITE OF POLYSTYRENE AND POLYHEDRAL OLIGOMERIC SILSESQUI-OXANE) อ.ที่ปรึกษาวิทยานิพนธ์หลัก: รศ.ดร.วรวีร์ โฮเว่น, อ.ที่ปรึกษาวิทยานิพนธ์ร่วม: ดร.วรล อินทสันตา, 62 หน้า

พอลิฮีดรัลโอลิโกเมอริกซิลเสสควิออกเซน (POSS) เป็นสารประกอบไฮบริดอินทรีย์-อนินทรีย์ มีสูตรทั่วไปคือ $(RSiO_{1.5})_n$ และมีโครงสร้างหลายแบบ POSS จึงมีศักยภาพในการนำไปประยุกต์ใช้หลายด้านโดยเฉพาะอย่างยิ่งที่เกี่ยวข้องกับพอลิเมอร์คอมพอสิต งานวิจัยนี้สังเคราะห์โคพอลิเมอร์แบบสุ่มและแบบบล็อกจากสไตรีนและเฮปทาไอโซบิวทิล-1-โพรพิลเมทาคริเลต)-พอลิฮีดรัลโอลิโกเมอริกซิลเสสควิออกเซน (MAPOSS) จากการทดลองพบว่าปฏิกิริยาพอลิเมอไรเซกลไกเป็นอนุมูลอิสระที่เป็นกระบวนการร่วม Activator Regenerated by Electron Transfer for Atom Transfer Radical Polymerization และ Reversible Addition-Fragmentation Chain Transfer (concurrent ARGET ATRP-RAFT) มีประสิทธิภาพสูงสุดในการสังเคราะห์โคพอลิเมอร์ที่สามารถควบคุมน้ำหนักโมเลกุลและการกระจายตัวของน้ำหนักโมเลกุลได้ จากการเตรียมเส้นใยจากโคพอลิเมอร์ที่สังเคราะห์ได้ด้วยเทคนิคอิเล็กโทรสปินนิงโดยใช้ตัวทำละลายผสมระหว่างเททราไฮโดรฟิวแรน (THF) และไดเมทิลฟอร์มาไมด์ (DMF) ในอัตราส่วนต่างๆ พบว่าเส้นใยพอลิสไตรีนมีการกระจายขนาดเส้นใยต่ำเมื่อขึ้นรูปจากตัวละลายผสม ในขณะที่เส้นใยจากโคพอลิเมอร์แบบสุ่มมีความขรุขระและความพรุนมากขึ้นตามสัดส่วนที่เพิ่มขึ้นของ DMF ในตัวทำละลายผสมและปริมาณของ MAPOSS โดยเชื่อว่าสัณฐานวิทยาดังกล่าวมีที่มาจากความสามารถในการละลายต่ำของเฟส MAPOSS ใน DMF นอกจากนี้ยังพบว่าในสภาวะการขึ้นรูปแบบเดียวกันโคพอลิเมอร์แบบบล็อกเกิดความขรุขระชัดเจนกว่าโคพอลิเมอร์แบบสุ่ม

ภาควิชา .... เคมี .... ลายมือชื่อนิสิต ....

สาขาวิชา .... เคมี .... ลายมือชื่อ อ.ที่ปรึกษาวิทยานิพนธ์หลัก ....

ปีการศึกษา .... 2554 .... ลายมือชื่อ อ.ที่ปรึกษาวิทยานิพนธ์ร่วม ....

\# \# 5272328323: MAJOR CHEMISTRY

KEYWORDS : POLYHEDRAL OLIGOMERIC SILSESQUIOXANE (POSS)/ POLYSTYRENE/ ELECTROSPINNING/ PHASE SEPERATION

THANARATH PISUCHPEN: FIBER FROM POLYMER COMPOSITE OF POLYSTYRENE AND POLYHEDRAL OLIGOMERIC SILSESQUI-OXANE. ADVISOR: ASSOC. PROF. VORAVEE P. HOVEN, Ph.D., CO-ADVISOR: VAROL INTASANTA, Ph.D., 62 pp.

Polyhedral oligomeric silsesquioxane (POSS) is an organic-inorganic hybrid compound with an empirical formula of $(RSiO1.5)_n$ and various structural formulas possesses a great potential in many applications, especially in the area of polymer composites. Here in this research, random and block copolymers of styrene and heptaisobutyl-(1-propylmethacrylate)-POSS (MAPOSS) or PS-co-PMAPOSS were synthesized. Among all living polymerization routes tested, Concurrent Activator Regenerated by Electron Transfer for Atom Transfer Radical Polymerization and Reversible Addition-Fragmentation Chain Transfer (concurrent ARGET ATRP-RAFT) was the most efficient one that yielded copolymers with controllable molecular weight and polydispersity. Fiber mats of the selected copolymers were then fabricated by electrospinning using mixed solvent of tetrahydrofuran (THF) and dimethylformamide (DMF). For PS, fiber with low diameter distribution could be obtained with mixed solvent of THF/DMF. For PS-r-PMAPOSS, however, an increase of DMF content in the mixed solvent of THF/DMF resulted in porous fibers with rough surface, degree of which also depended upon the MAPOSS content. Poor solubility of MAPOSS phase in DMF seemed to be an origin of these morphological features. Under the same electrospinning condition, fibers from the block copolymer were apparently rougher than that from the random copolymer.

Department: .... Chemistry .... Student's signature.........................

Field of Study: .... Chemistry .... Advisor's signature.........................

Academic Year:.................... 2011 .... Co-advisor's signature.........................

ACKNOWLEDGEMENTS

CONTENTS

LIST OF TABLES

LIST OF FIGURES

Figure   Page

Figure   Page

LIST OF SCHEMES

LIST OF ABBREVIATIONS

ACVA : 4,4'-azobis-(4-cyanovaleric acid)

ARGET ATRP : activator regenerated by electron transfer for atom transfer radical polymerizarion

ATRP : atom transfer radical polymerizarion

CVADTB : 4-cyano-4-(thiobenzoylthio)pentanoic acid (4-cyanovaleric acid dithiobenzoate)

DMF : *N,N*-dimethylformamide

EBiB : ethyl α-bromoisobutyrate

MAPOSS : heptaisobutyl(1-propylmethacrylate)-POSS

Me$_6$TREN : tris[2-(dimethylamino)ethyl]amine

M$_n$: number average molecular weight

M$_w$: weight average molecular weight

PDI : polydispersity Index

PMDETA : *N,N,N',N'',N''*-pentamethyldiethylenetriamine

POSS : Polyhedral Oligomeric Silsesquioxane

PS : polystyrene

Sty : styrene

THF : tetrahydrofuran

CHAPTER I

INTRODUCTION

1.1 Statement of Problem

Polyhedral oligomeric silsesquioxane (POSS) is an organic-inorganic hybrid compound with an empirical formula of $(RSiO_{1.5})_n$ with R as hydrogen, alkyl, aryl or other functional groups and various structural formulas. Due to its similarity to silica, POSS can sometimes be referred to the smallest colloidal silica. As its physical and chemical properties can be varied with alkyl groups, POSS possesses a great potential in many applications, especially in the area of polymer composites [1]. Direct addition of POSS can only be possible at low level, as high amount of POSS incorporation can lead to phase separation of POSS from the matrix [2-4]. Attaching POSS to polymer via either grafting or copolymerization offers an alternative way to improve POSS distribution, and may perhaps lead to different composite morphologies [2,3].

Electrospinning is a simple and versatile technique that can be used to fabricate polymer solution into non-woven fiber mat using coulombic force. It is also capable of generating polymer composite having distinctive morphology and facilitate POSS incorporation into polymer matrix without causing POSS aggregation [5,6]. Here in this research, we are interested to produce fibers from copolymers containing POSS using electrospinning. Copolymers of commercially available heptaisobutyl-(1-propylmethacrylate)-POSS (MAPOSS) and styrene were synthesized by living polymerization methods. The efficiency of polymerization methods was determined based on the control of molecular weight and polydispersity index. Effects of solvent and MAPOSS content in the copolymer on fiber morphology were also evaluated.

1.2 Objective

1.2.1 To synthesize and characterize random and block copolymers of styrene and MAPOSS

1.2.2 To fabricate the electrospun fiber mat from copolymer of styrene and MAPOSS

1.3 Scope of Investigation

The stepwise investigation was carried out as follows.

1. Literature survey for related research work

2. Synthesis of polystyrene (PS) and both random and block copolymers of styrene and MAPOSS (PS-*co*-PMAPOSS)

3. Characterization of copolymers by ^{1}H-NMR and GPC

4. Preparation of PS and PS-*co*-PMAPOSS fiber mats by electrospinning

5. Characterization of PS and PS-*co*-PMAPOSS fiber mats by SEM, XRD, and AFM

CHAPTER II

THEORY AND LITERATURE REVIEW

2.1 Polyhedral Oligomeric Silsesquioxane

2.1.1 Chemical Properties

The term silsesquioxane refers to any organic-inorganic hybrid compounds with an empirical formula of $(RSiO_{1.5})_n$. R groups are hydrogen, alkyl, aryl, or other function groups. Silsesquioxane can be in the form of random structure, laddered, partial caged, and complete caged structure with various geometries (**Figure 2.1**). The first oligomeric organosilsesquioxanes, $(CH_3SiO_{1.5})_n$, were isolated along with other volatile compounds by Scott in 1946 through thermolysis of the polymeric products obtained from methyltrichlorosilane and dimethylchlorosilane cohydrolysis [1].

Random   Ladder   Partial Cage

Cage

T4   T6   T8   T10   T12
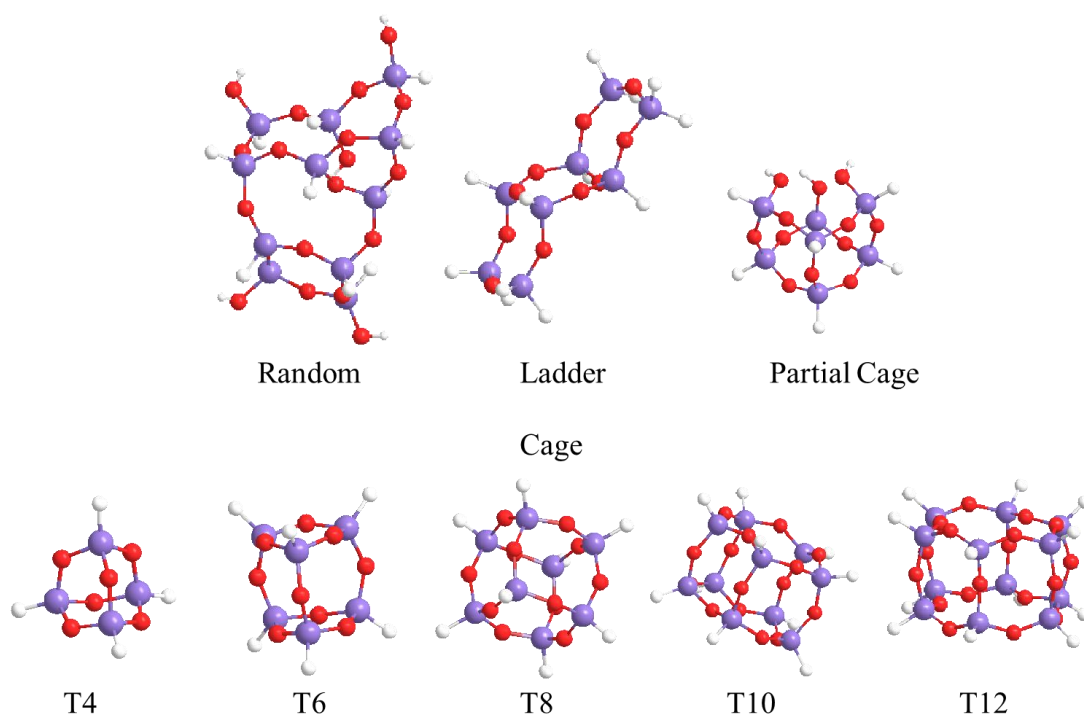
Figure 2.1 Various structures of POSS.[1]

Nanostructure of POSS, with sizes of 1 to 3 nm in diameter, can be thought of as the smallest possible particles of silica. Each POSS molecule contains organic substituents (R groups) on its outer surface that make it compatible with polymers, biological systems, or surfaces and can be designed to be nonreactive or reactive. POSS is also non-volatile, which make it odorless.

2.1.2 Application in Polymer Composite

POSS can be incorporated into polymers via blending or, in case of functional POSS, grafting onto polymer chain or copolymerization with other monomer. The incorporation of POSS derivatives into polymeric materials can lead to improvements in polymer properties which include, but are not limited to, increase in use temperature, oxidation resistance, surface hardening, and improved mechanical properties, as well as reduction in flammability, heat evolution, and viscosity during processing. The examples are as followed:

In 2002, Zhang *et al*. [2] prepared random copolymer of methyl methacrylate (MMA) and heptacyclopentyl-(1-propylmethacrylate)-POSS (MAPOSS) with atom transfer radical polymerization (ATRP) method. Synthesized copolymers were used in PS-PMMA blend in which copolymers helped increasing compatibility between two polymer phases which led to better polymer phase distribution and stability at high temperature as can be seen in **Figure 2.2**.
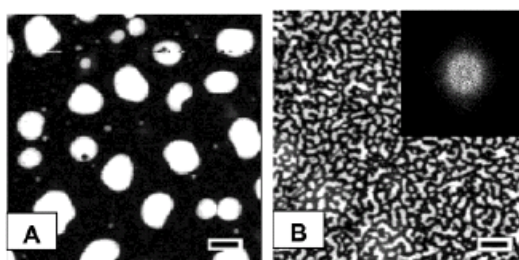
Figure 2.2 TEM micrographs of PS-PMMA polymer blend (A) and PS-PMMA and PMMA-*r*-PMAPOSS polymer blend.[2]

In 2006, Joshi *et al.* [3] prepared high density polyethylene (HDPE)-octamethyl-POSS nanocomposites by melt mixing. The rheological and viscoelastic behavior of HDPE-octamethyl-POSS nanocomposites was investigated with a strain-controlled rheometer and dynamic mechanical analysis (DMA). The results showed that the low amount of POSS acted as lubricant and reduce the complex viscosity of the nanocomposites, increase in storage modulus, and transition temperature. The high content of POSS, on the other hand induced an increase in viscosity and decrease in storage modulus. POSS remained miscible in HDPE at lower concentration and temperature but began to aggregate at higher concentration and temperature. Gelation of HDPE also occurred at concentration higher than 5 wt% possibly due to the segregated particle-particle interaction.

In 2007, Kim *et al.* [4] prepared poly(vinyl alcohol) (PVA)-POSS composite by grafting heptacyclohexyl(isocyanatopropyldimethylsilyl)-POSS onto PVA chain through urethane linkage (-NH-COO-). Addition of POSS containing hydrophobic cyclohexyl groups to hydrophilic PVA reduced solubility in water and prevented electrospun fiber from PVA-POSS composite from dissolving in water (**Figure 2.3c-d**).
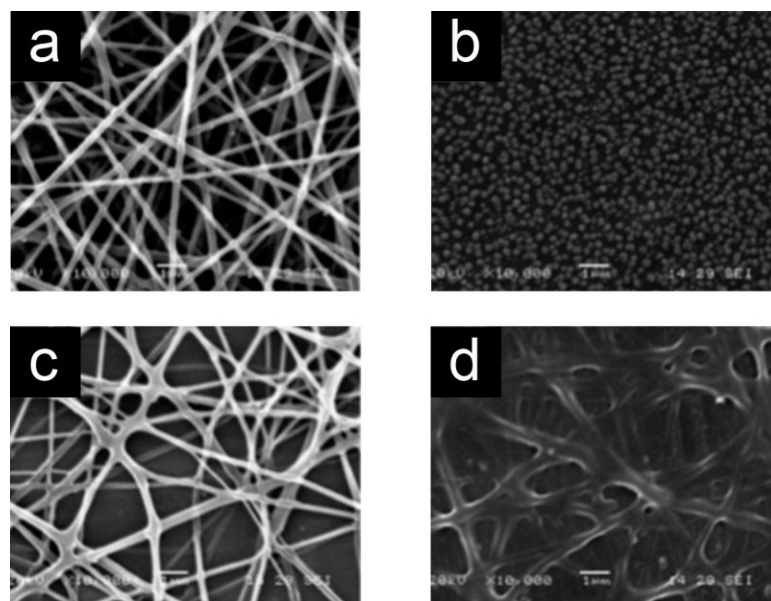
Figure 2.3 SEM micrograph of PVA fiber before (a) and after (b) contact with water and PVA-POSS composite fiber before (c) and after (d) contact with water.[4]

In 2009 Zhang *et al*. [7] synthesized tadpole-shaped poly(tert-butyl acrylate) (PtBA) using a POSS-containing chain transfer agent (CTA) through Reversible Addition-Fragmentation Chain Transfer Polymerization (RAFT). POSS-PtBA was further hydrolyzed into amphiphilic, tadpole-shaped poly(acrylic acid) (POSSPAA), which self-assembled in water into rather large aggregates where the POSS moieties are dispersed in the particle (**Figure 2.4**). The size was nearly independent of the chain length of PAA but pH-responsive due to the presence of carboxyl groups on PAA chains.
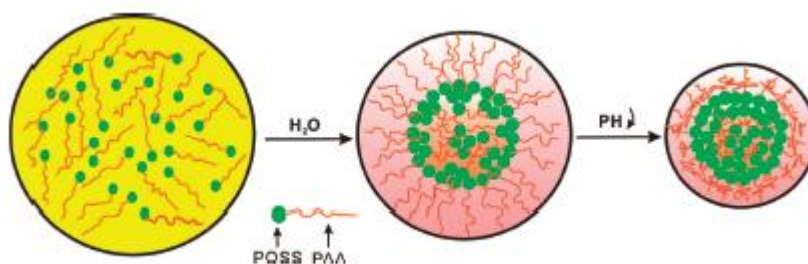
Figure 2.4 Self-assembly process in POSS-containing PAA in aqueous solution.[7]

In 2011, Gu *et al*. [8] synthesized poly(ε-caprolactone) (PCL), poly(ethylene glycol) (PEG) and POSS multiblock copolymer using urethane linkage from lysine-derived diisocyanate. POSS incorporation had been found to suppress *in vitro* enzymatic hydrolytic degradation of PCL-PEG-based multiblock thermoplastic polyurethane by a surface passivation mechanism (**Figure 2.5**). Wavelength Dispersive X-Ray Spectrometry (WDS revealed that the covalently bonded POSS moieties developed a near-continuous and robust POSS-layer after initial degradation, which prevented ester bonds of PCL from enzymatic attack, thereby inhibiting further degradation. This phenomenon was not found in physically blended POSS composite.
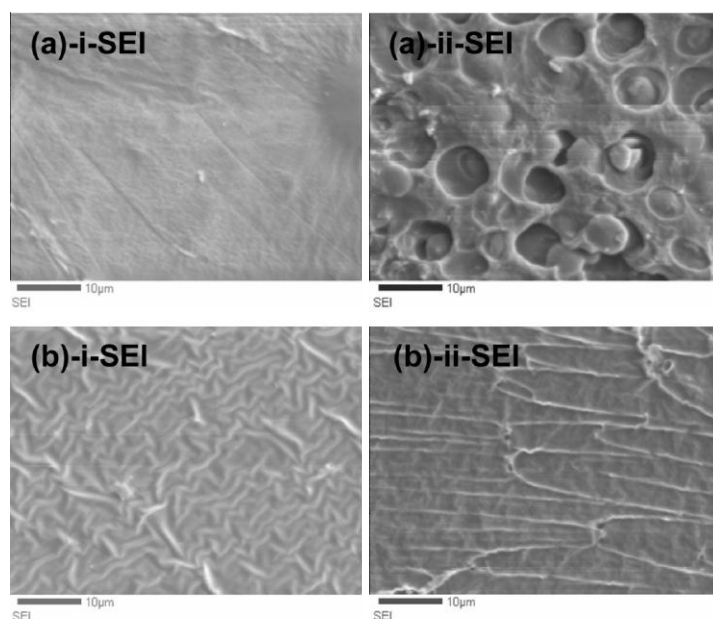
Figure 2.5 SEM micrographs of physically blended PCL-PEG-POSS composite before (a-i) and after (a-ii) hydrolysis by lipase and PCL-PEG-POSS multiblock copolymer before (b-i) and after (b-ii) hydrolysis by lipase.[8]

2.2 Electrospinning Process [9]

Electrospinning is a unique process of fabrication of ultrafine fiber using coulombic force from a high voltage electrical field. Similar to electrospray, polymer solution or melt is drawn out of syringe through coulombic force. Unlike electrospray, however, viscous polymer solution or melt is stretched to create an electrically charged jet, which dries or solidifies to leave a polymer fiber.

The electrospinning process can be described thusly: when a high voltage is applied to a polymer solution, a high electric field is generated between a polymer fluid (contained in a spinning dope reservoir with a capillary tip or a spinneret) and a metallic fiber collection ground surface. As the intensity of the electric field is increased, the hemispherical surface of the fluid at the tip of the capillary tube is distorted into a conical shape known as the Taylor cone. Further increasing the electric field past a threshold causes the repulsive electrostatic force to overcome the surface tension and the charged jet of the fluid is ejected from the tip of the Taylor cone. The electrically charged jet undergoes a stretching and whipping process

leading to the formation of long narrow thread. This stretching process is accompanied by the rapid evaporation of the solvent molecules, further reducing the diameter of the polymer jet. The dry fibers are then collected on the collection plate, resulting in a non-woven mesh of nano-to-micro diameter fibers. A schematic drawing of the electrospinning process is shown in **Figure 2.6**.
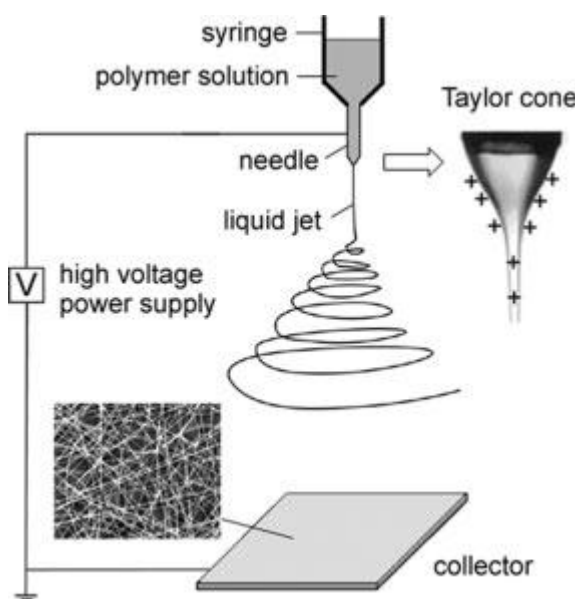
Figure 2.6 Schematic diagram shows polymer nanofibers forming by electrospinning process.[9]

The properties of fiber obtained from this process depend on two parameters; the first is the property of the polymer solution, including the type of polymer, molecular weight, chain conformation, viscosity (or concentration), conductivity and surface tension of solvent. The second one is equipment setup parameters including electrical field strength, flow rate, collection distance, and ambient parameters (temperature, humidity and air velocity in the chamber).

The advantages of electrospinning process are simple equipment, requiring a short time, cost effective process and producing a very high orientation fiber with very small pore sizes. Therefore, electrospun fibers from electrospinning have regained more attention probably due in part to interest in many applications such as in the field of filtration systems [10], medical prosthesis mainly grafts and vessels,

tissue template [11], electromagnetic interference shielding [12], protective clothing [13], composite delamination resistance , and chemical and biochemical sensors [14].

2.3 Electrospinning for Polymer-POSS Composite

Electrospinning is a powerful technique to make ultrafine fibers and capable of generating polymer composite having distinctive morphology and facilitate POSS incorporation into polymer matrix without causing POSS aggregation. The examples of related research work are as followed:

In 2007, Tuteja *et al.* [15] fabricated superhydrophobic electrospun fiber mat from composite of PMMA and octaperfluorodecyl-POSS. Wettability of the fiber mat also depended on octaperfluorodecyl-POSS content, being superoleophilic at low octaperfluorodecyl-POSS content, and superoleophobic at high octaperfluorodecyl-POSS content. This characteristic rendered the fiber mat to be used for water-organic compound separation.

In 2009, Xue *et al.* [5] fabricated electrospun fiber mat from random copolymer of PMMA and heptaisobutyl-(1-propylmethacrylate)-POSS (MAPOSS) which exhibited superhydrophobicity. Unlike the PMMA fiber (**Figure 2.7a**), the random copolymer (PMMA-r-PMAPOSS) also showed major nanofibrilar sub-structure (**Figure 2.7b**).
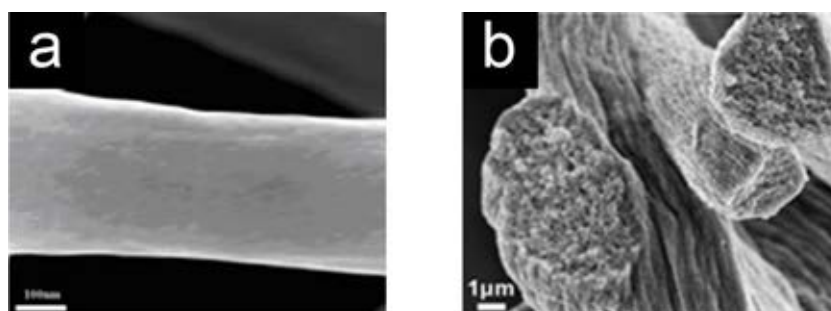
Figure 2.7 SEM micrographs of electrospun PMMA (a) and PMMA-r-PMAPOSS (b) fibers. [5]

In 2010, Cozza *et al.* [6] prepared cellulose acetate (CA) grafted with epoxy-POSSS (MAPOSS) yielding CA-POSS. They have demonstrated that POSS domain distributed evenly when the modified polymer was fabricated into electrospun fiber (**Figure 2.8b**), but phase aggregated when it was fabricated into film (**Figure 2.8a**). Rapid evaporation of solvent during fiber stretching was the major factor that prevented aggregation of POSS.
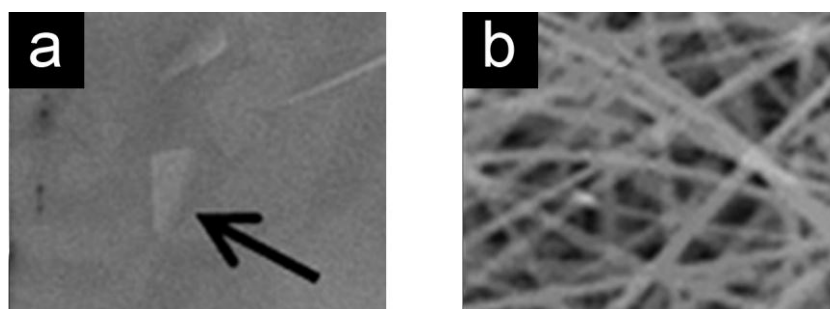
Figure 2.8 SEM micrographs of CA-POSS in the form of casted film (a) and electrospun fiber (b). [6]

2.4 Polystyrene (PS)

Polystyrene (PS), a non-polar polyphenyl synthetic polymer, has been used since 1931 [16] in a wide range of industrial and commercial applications because of its excellent chemical resistance and physical properties, some of which are shown in the **Table 2.1**.

Table 2.1 General chemical identity and physical properties of polystyrene

Identity/Properties	Detail
Structure formula	$(-CH_2-CH(C_6H_5)-)-_m$
Physical appearance	White powder or colorless pellet
Glass Transition Temperature	$100^{\circ}C$
Melting Point	$240^{\circ}C$
Specific gravity	1.05
Solubility	Insoluble in water and alchohol, soluble in ether, acetone, DMF, chloroform

Polystyrene (PS) is used for producing plastic model assembly kits, plastic cutlery, CD "jewel" cases, smoke detector housings, license plate frames, and many other objects where a fairly rigid, economical plastic is desired. Another common utility of PS is PS foam, which is light-weighted and has good thermal insulation and damping property, make it is widely used as insulator and packaging. On the other hand, its chemical inertness is an obstacle in the modification of PS for further application, usually requires drastic reaction such as sulfonation, nitration, or plasma treatment. Its hydrophobicity and phenyl group also make PS not biocompartible without extra treatment.

2.5 Electrospinning of Polystyrene

There are many researchers reported that PS was successfully fabricated into electrospun fiber [17] which, due to its hydrophobicity and chemical inertness, could be used in various applications, as followed:

In 2006, Baker *et al*. [18] fabricated argon plasma-treated electrospun polystyrene scaffold which could be used in cell culture experiment. Smooth muscle cells (SMC) were cultured on the scaffold to determine its applicability for cell culture. It was found that the alignment factors of the actin filaments were 0.19 and 0.74 for the random and aligned scaffold respectively, as compared to 0.51 of the native tissue. The results suggested that polystyrene scaffolds promoted and induced alignment in growth of collagen fibers.
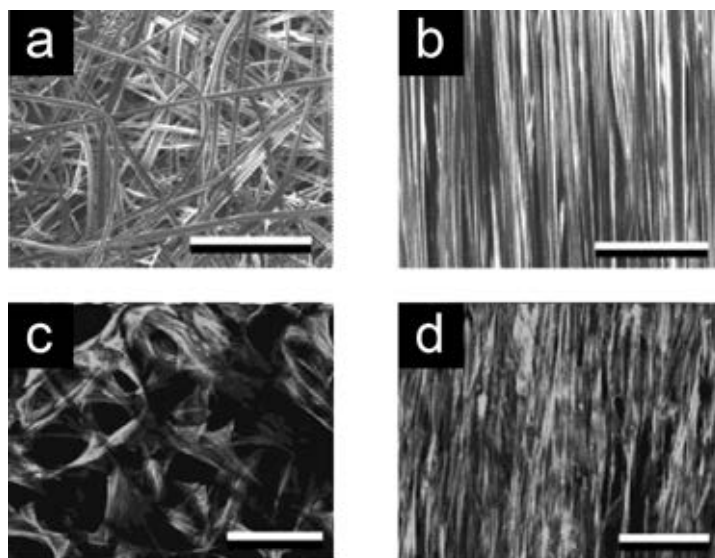
Figure 2.9 SEM micrographs of random (a) and aligned (b) PS scaffold and confocal micrographs of human bladder SMC cultured for 48 hours on random (c) and aligned (d) PS scaffold. Scale bar = 20 μm [18]

In 2006, Zhu *et al.* [19] fabricated electrospun fiber mat of composite between conducting polymer polyaniline (PANI) and PS. The resulting surface was superhydrophobic with water contact angle of 162° and very small sliding angle (**Figure 2.10** b-c). Moreover, due to chemical inertness of PS, both superhydrophobicity and conductivity of PANI/PS fiber mat was not affected by pH or oxidizing agent, such as ammonium persulfate, and remained stable for several months.
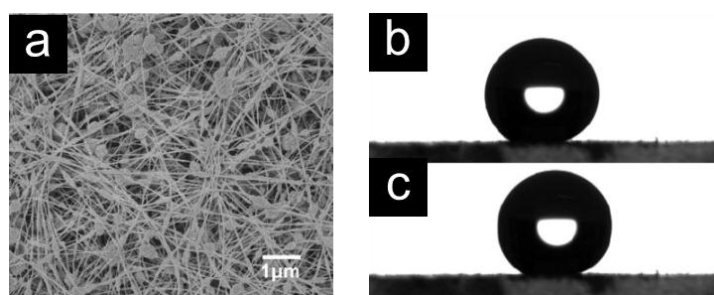
Figure 2.10 SEM micrograph of PANI/PS fiber mat (a) and photographs of water droplet before (b) and after (c) sliding on PANI/PS fiber mat. [19]

In 2008, Wang *et al.* [20] fabricated poly(*N*-isopropylacrylamide) (PNIPAAM)/PS composite electrospun fiber. Due to thermoresponsive property of PNIPAAM and hydrophobicity of PS, composite with PNIPAAM content of 20% (w/w) and above could switch between being superhydrophilic at temperature lower than lower critical solution temperature (LCST, 32-33°C for PNIPAAM) and superhydrophobic at temperature higher than LCST.
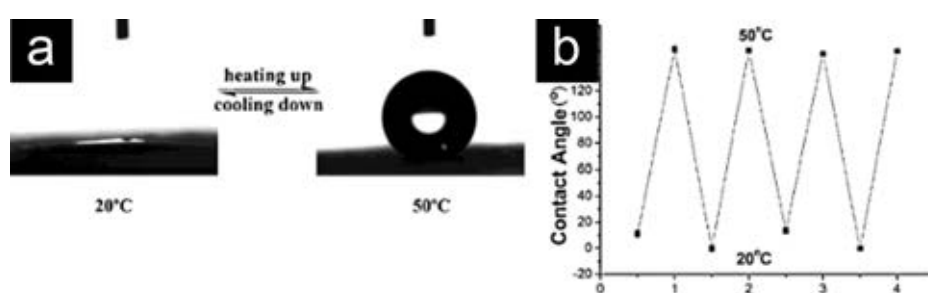
Figure 2.11 Photographs of water-droplet shape on thermoresponsive PNIPAAM/PS fiber mat (a) and reversibility of water contact angle transition on the PNIPAAM/PS fiber mat (b).[20]

2.6 Phase Separation in PolystyreneBlends and Composites

Making polymer blends and composite materials is a simple method to improve properties of polymer for applications. Being non-polar polymer, phase separation in polystyrene (PS) blend with polar polymer is to be expected. Phase separation in composite with inorganic material is also common scenario. The examples are as followed:

In 2004, Kailas *et al.* [21] studied the phase separation behavior of PS-PMMA blend thin film compared to PS-PMMA block copolymer thin film. Both types of film were spun-casted on silicon wafers and annealed at 160°C. Similar to the work reported by Zhang *et al.* [2] mentioned above, PS-PMMA blend was separated into multiple PS domains on PMMA film (**Figure 2.12a-b**), suggesting that non-polar PS detached from silicon wafer surface while PMMA covered the rest of surface. Phase separation was incomplete in the case of block copolymer.Only segregation of PS moiety on the surface and island-like morphology without apparent phase separation (**Figure 2.12c-d**).
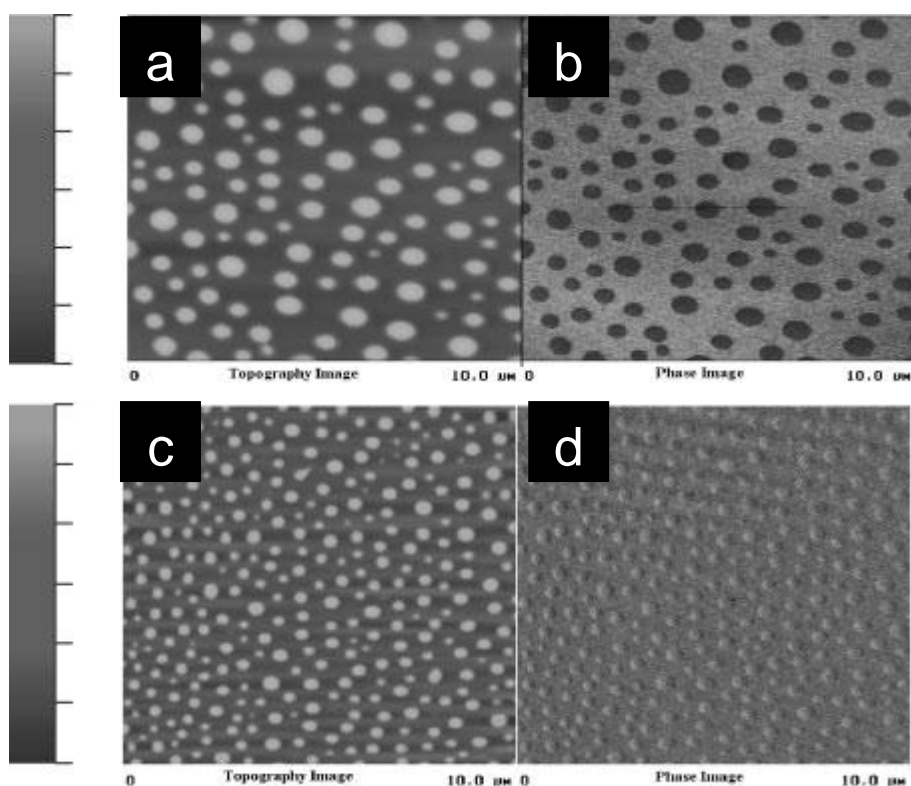
Figure 2.12 AFM topographical (a) and phase (b) images of PS-PMMA blend and AFM topographical (c) and phase (d) images of PS-PMMA block copolymer. Unit on the ruler is 5 nm. [21]

In 2006, Wei *et al*. [22] fabricated various electrospun polymer blend fibers, including PS-PMMA fiber. PS-PMMA with 2 molecular weights of PMMA (280 kDa for PS, 120 and 15 kDa for PMMA) was used in electrospinning. With high molecular weight PMMA, fibers with co-continuous structure were obtained (**Figure 2.13a**), having both PS and PMMA phases oriented along the fiber length. Low molecular weight PMMA, on the other hand, caused polymer blend to form core-sheath structure, with PS domain as core (**Figure 2.13b**). Core-sheath formation took place as a result of lowered viscosity or better solubility of low molecular weight PMMA.
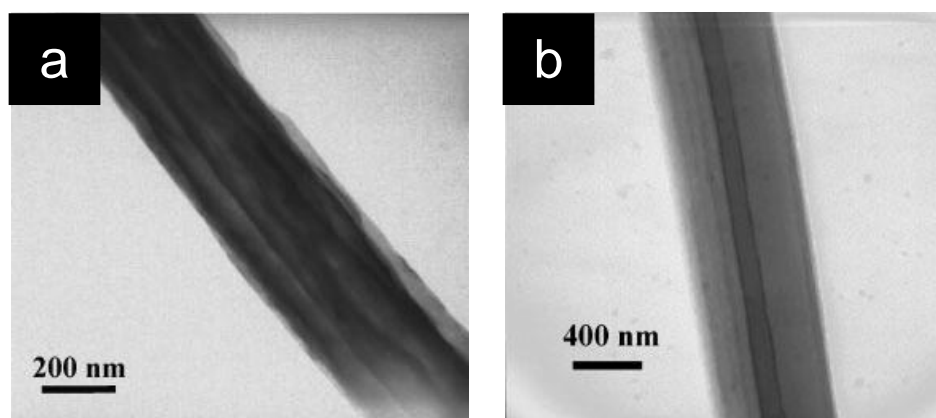
Figure 2.13 SEM micrographs of electrospun fiber of polymer blend of PS and high (a) or low (b) molecular weight PMMA. [22]

In 2008, Hirai *et al.* [23] synthesized PS-*b*-PMAPOSS and PMMA-*b*-PMAPOSS through living anionic polymerization using *sec*-BuLi and 1,1-diphenylethylene as initiating system. Analysis with transmission electron microscopy (TEM) revealed lamellar structure formed through phase separation of organic phase (PS or PMMA) and inorganic phase (MAPOSS).
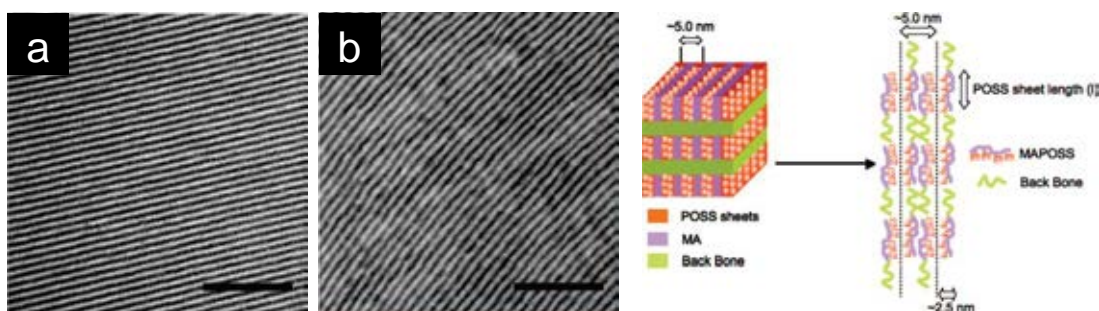
Figure 2.14 TEM micrograph of PMMA-*b*-PMAPOSS (a) and PS-*b*-PMAPOSS (b) film and schematic illustration of lamellar structure. [23]

2.7 Living Polymerization

Normally, chain polymerization has 3 parts: initiation, propagation, and termination. Because termination can occur through many means (combination, chain transfer, disproportionation), control of molecular weight and synthesis of "block-copolymer" is hard to achieve through normal mean. Living polymerization

is a form of chain polymerization where the ability of a growing polymer chain to terminate has been removed. Instead, polymerization intermediate is converted to "inactive form" to stop polymerization while allow future growth. Chain termination and chain transfer reactions are absent and the rate of chain initiation is also much larger than the rate of chain propagation. The result is that the polymer chains grow at a more constant rate than seen in traditional chain polymerization and have a very low polydispersity index [24].

2.7.1 Atom Transfer Radical Polymerization [25]

Atom transfer radical polymerization (ATRP) is an example of a living polymerization. As the name implies, the atom transfer step is the key step in the reaction responsible for uniform polymer chain growth. The uniform polymer chain growth stems from the transition metal based catalyst. This catalyst provides an equilibrium between active polymer (radical intermediate) and an inactive form (alkyl halide) of the polymer; known as the dormant form. Since the dormant state of the polymer is vastly preferred in this equilibrium, the concentration of propagating radical is lowered, therefore suppressing unintentional termination and controlling molecular weights.
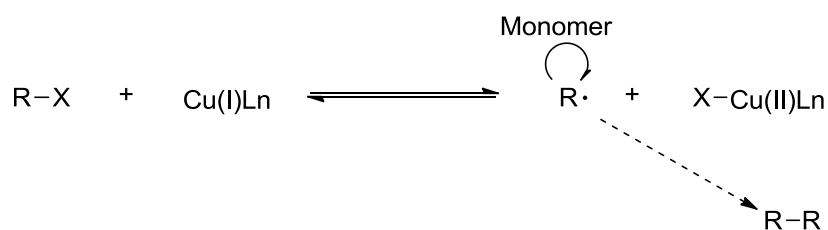
Scheme 2.1 Reaction mechanism of ATRP.

2.7.2 Activator Regenerated by Electron Transfer for Atom Transfer Radical Polymerization [26]

Despite being one of effective living polymerization, ATRP still has some disadvantages in term of catalyst. Cu(I) catalyst would be inevitably lost due to termination of polymer chain (shift equilibrium toward radical and Cu(II)) and other side reactions, thus initial amount of Cu(I) must be high enough to last through the whole reaction. This requires removal of catalyst after reaction, which is not

practical for industrial utilization. Activator Regenerated by Electron Transfer (ARGET) ATRP is an improvement of original ATRP technique by introduction of reducing agent, which continuously regenerate Cu(I) complex, allow lower amount of catalyst need for polymerization while provide efficient control of polymerization.
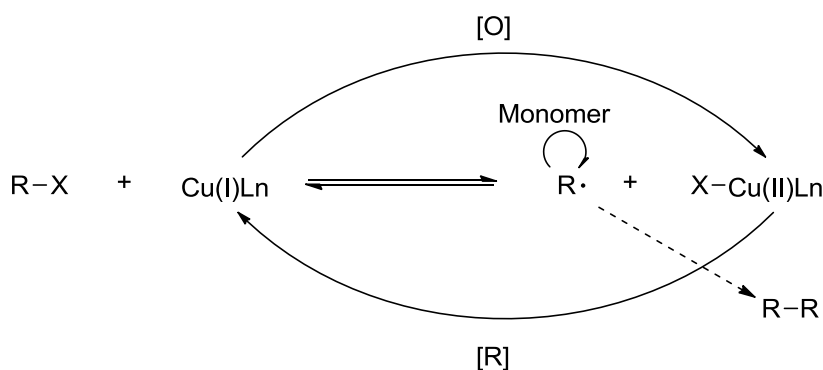
Scheme 2.2 Reaction mechanism of ARGET ATRP.

2.7.3 Reversible Addition Fragmentation Chain Transfer (RAFT) Polymerization [27]

Another method of living polymerization with good efficiency and versatility is RAFT polymerization. The RAFT process involves free radical polymerization in the presence of dithioesters reagent. The usual azo or peroxy initiators are employed. The mechanism of RAFT polymerization involves a reversible addition-fragmentation sequence in which S=C(Z)S- moiety is transferred between active and dormant chains that help maintaining the living character of the polymerization. The effectiveness of dithioester compound is attributed to their very high transfer constants which ensure a rapid rate of exchange between dormant and living chains. A major advantage of the RAFT polymerization is its compatibility with a wide variety of monomers.

Scheme 2.3 Reaction mechanism of RAFT polymerization.

2.7.4 Concurrent Reversible Addition-Fragmentation Chain Transfer - Activator Regenerated by Electron Transfer for Atom Transfer Radical Polymerization [28]

While ATRP mechanism normally relies on atom transfer reaction of halide atom, it was found that other functional group, including dithioester, can react with metal complex in the same fashion with alkyl halide that generates radical [29]. Unlike normal RAFT, which requires external source of radical, atom transfer process provides the consistent amount of radical which is under control by both ATRP and RAFT equilibria, providing a better control. An addition of reducing agent as in ARGET ATRP further reduces amount of catalyst required, which minimizes the chance of side reactions and makes removal of catalyst easier or negligible. Solid reducing agent, such as copper wire for Cu(II) complex, allows easier handling and removal [30].
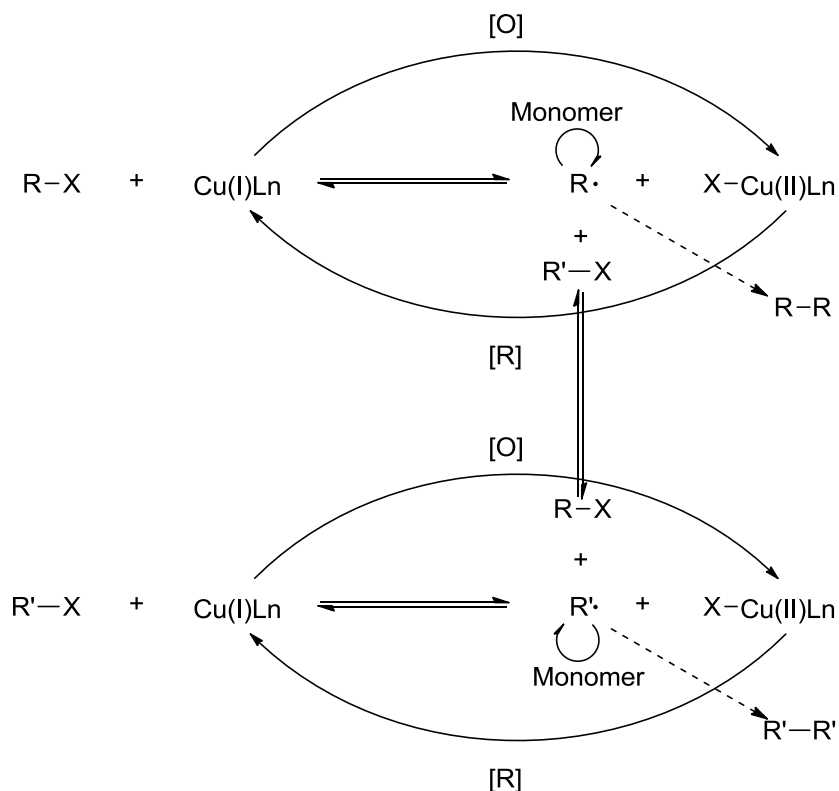
Scheme 2.4 Reaction mechanism of concurrent RAFT-ARGET ATRP.

CHAPTER III

EXPERIMENTAL

3.1 Materials

All reagents and materials are analytical grade (unless stated otherwise) and used without further purification.

1. Styrene (Sty)	: Fluka
2. Methyl methacrylate	: Fluka
3. Heptaisobutyl (1-propylmethacrylate)-POSS (MAPOSS)	: Sigma-Aldrich
4. *N,N,N'N'',N''*-Pentamethyldiethylenetriamine	: Aldrich
5. Copper(I) Bromide	: Fluka
6. Copper(II) Bromide	: Fluka
7. Ethyl α-bromoisobutyrate(EBiB)	: Fluka
8. 4,4′-Azobis(4-cyanovaleric acid)(ACVA)	: Sigma-Aldrich
9. 4-Cyano-4-(phenylcarbonothioylthio)pentanoic acid (CVADTB)	: Sigma-Aldrich
10. Copper(0) Wire	
11. Aluminium Oxide	: Sigma-Aldrich
12. Toluene	: Lab-scan
13. Tetrahydrofuran (THF)	: Lab-scan
14. *N,N*-Dimethylformamide (DMF)	: Lab-scan
15. Ethanol	: Lab-scan

3.2 Equipment

3.2.1 Nuclear Magnetic Resonance Spectroscopy (NMR)

The ^{1}H-NMR spectra was recorded in CDCl$_3$ using Varian, model Mercury-400 nuclear magnetic resonance operating at 400 MHz. Chemical shift (δ) are reported in part per million (ppm) relative to tetramethylsilane (TMS) or using the residual protonated solvent signal as reference**.**

3.2.2 Gel Permeation Chromatography (GPC)

The molecular weight and molecular weight distribution of synthesized (co)polymers were determined by gel permeation chromatography (GPC) using Water 600 controller and pump, Waters E600 column connected to Waters 2140 refractive index detector, and THF as eluent. The flow rate was 1 mL/min. Narrow PS standards were used for generating calibration curve.

3.2.3 Thermogravimetric Analysis (TGA)

The thermal degradation behavior of all (co)polymer samples and the weight ratio of ash were investigated by thermogravimetric analysis (TGA) (Mettler Toledo, model TGA/SDTA 851 USA) over a temperature range of 30-600 ∘C at a heating rate of 10 ∘C /min under ambient condition. The data were analyzed with STARe SW program version 9.30.

3.2.4 Scanning Electron Microscopy (SEM) and Energy Dispersive X-Ray Spectrometry (SEM-EDS)

The morphological appearances of the as-spun fibers were investigated using a scanning electron microscope (SEM, JEOL, Model JSM-6480LV, Japan). Each sample was placed on the holder with an adhesive tape and coated with a thin layer of gold. The scanning electron images were obtained by using an acceleration voltage of 15kV. The average fiber diameter of the electrospun fibers was measured by Semafore software directly from SEM images. For analysis of elemental composition, the as-spun fibers were investigated using a scanning electron microscope (SEM) model JSM-5800LV(JEOL, Japan).

3.2.5 X-ray Diffractometry (XRD)

The crystallinity of the synthesized (co)polymers and as-spun fibers were investigated using a X-ray diffractometer (model Rigaku TTRAX III, 18kW, Japan). Each sample was ground into powder prior to analysis.

3.3 Synthesis of Polystyrene (PS)

3.3.1 Atom Transfer Radical Polymerization (ATRP)
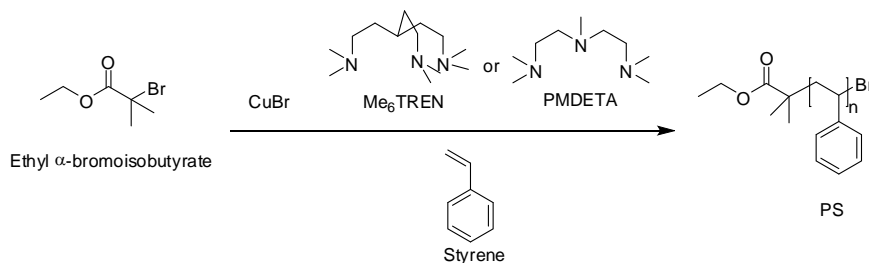
CuBr (72 mg, 0.5 mmol), Me$_6$TREN (134 µL, 0.5 mmol) or PMDETA (134 µL, 0.6 mmol) and Sty (5.7 mL, 0.05 mol) were added into a 10 mL scintillation vial, which was then sealed with rubber septum. After being purged with nitrogen gas for 15 minutes, EBiB having designated mole ratio (**Table 3.1**) mixed with 1.5 mL toluene was added via purged syringe. The reaction was carried out under nitrogen atmosphere at 110 °C for 24 hours.

Table 3.1 Molar ratio of reagent used in the synthesis of PS using ATRP method

Ligand	CuBr:Ligand:EBiB	Sty:EBiB
	1:1:1	100:1
Me$_6$TREN	1:1:0.5	200:1
	1:1:0.2	500:1
PMDETA	1:1.2:1	100:1
	1:1.2:0.2	500:1

3.3.2 Activator Regenerated by Electron Transfer for Atom Transfer Radical Polymerization (ARGET ATRP)
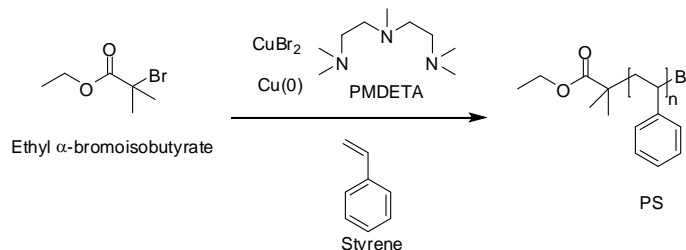
CuBr$_2$ (2 mg, 0.008 mmol), copper wire (4.8 g, 0.076 mol), PMDETA (26 µL, 0.12 mmol) and Sty (5.7 mL, 0.05 mol) were added into a 10 mL scintillation vial, which was then sealed with septum. After being purged with nitrogen gas for 15 minutes, EBiB mixed with 1.5 mL toluene was added via purged syringe. Molar ratio of CuBr$_2$:PMDETA:EBIB and Sty:EBiB were 1:140:11 and 500:1, respectively. The reaction was carried out under nitrogen atmosphere at 110 °C for 24 hours.

3.3.3 Reversible Addition-Fragmentation Chain Transfer (RAFT) Polymerization
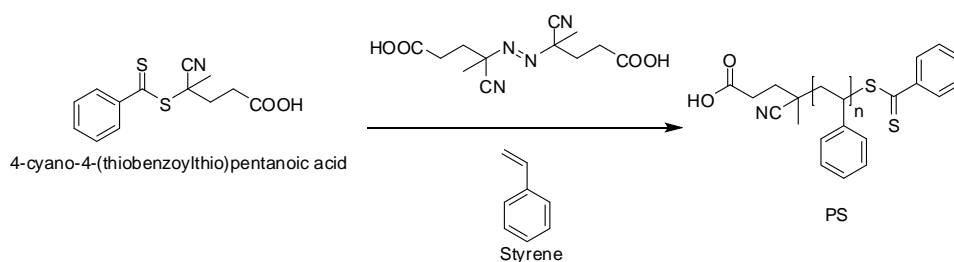
CVADTB (24 mg, 0.086 mmol), ACVA (3 mg, 0.011 mmol), and 13 mL of styrene (13 mL, 0.11 mol), (molar ratio of 8:1:10000) were added into a 25 mL scintillation vial, which was then sealed with rubber septum. After being purged with nitrogen gas for 15 minutes, the reaction was carried out under nitrogen atmosphere at 90 °C for 24 hours.

3.3.4 Concurrent Reversible Addition-Fragmentation Chain Transfer - Activator Regenerated by Electron Transfer for Atom Transfer Radical Polymerization (Concurrent RAFT-ARGET ATRP)

4-cyano-4-(thiobenzoylthio)pentanoic acid

Styrene

PS
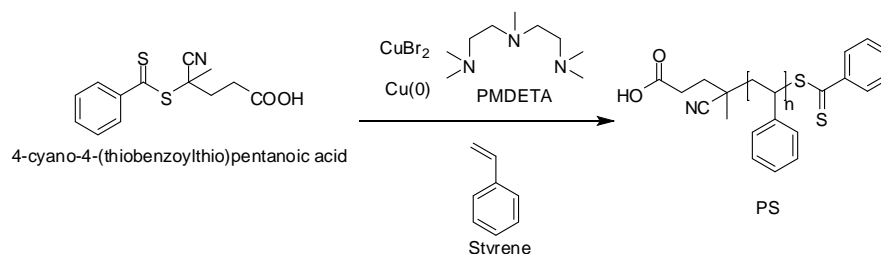
CuBr$_2$ (2 mg, 0.008 mmol), PMDETA (26 μL, 0.12 mmol), CVADTB (12 mg, 0.043 mmol), Sty (molar ratio of CuBr$_2$:PMDETA:CVADTB = 1:140:5 and Sty:CVADTB = 500:1, 1000:1 or 1300:1) and copper wire (4.8 g, 0.076 mol) were added into a 25 mL scintillation vial, which was then sealed with septum. After being purged with nitrogen gas for 15 minutes, the reaction was carried out under nitrogen atmosphere at 90∘C for 24 hours.

3.4 Synthesis of Copolymers of MAPOSS and Styrene (PS-*co*-PMAPOSS)
3.4.1 Random Copolymer (PS-*r*-PMAPOSS)
3.4.1.1 ATRP

EBIB

Me$_6$TREN   PMDETA

Styrene

MAPOSS

PS-*r*-PMAPOSS
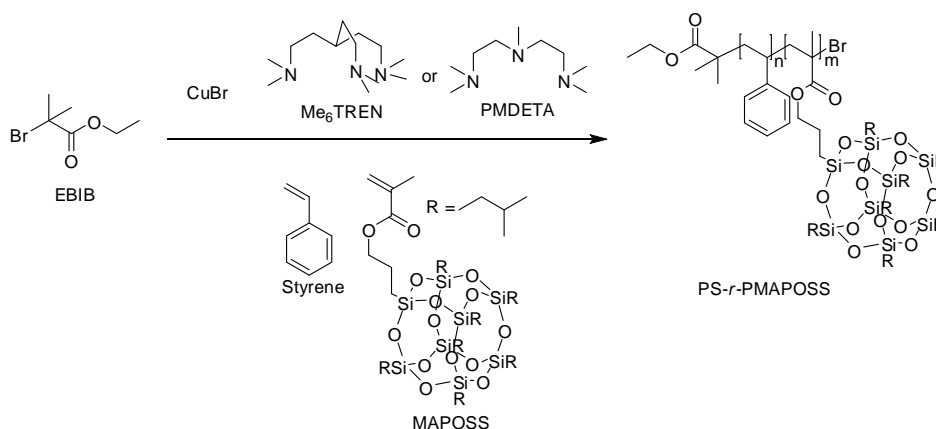
CuBr (72 mg, 0..5 mmol), Me$_6$TREN (134 μL, 0.5 mmol) or PMDETA (134 μL, 0.6 mmol), Sty (5.7 mL, 0.05 mol) and MAPOSS having designated mole ratio (**Table 3.2**) were added into a 10 mL scintillation vial, which was then sealed with rubber septum. After being purged with nitrogen gas for 15 minutes, EBiB having designated mole ratio (**Table 3.2**) mixed with 1.5 mL toluene was added via purged

syringe. The reaction was carried out under nitrogen atmosphere at 110 °C for 24 hours.

Table 3.2 Molar ratio of reagent used in the synthesis of PS-*r*-PMAPOSS using ATRP method

Ligand	CuBr:Ligand:EBiB	Sty:MAPOSS:EBiB
Me$_6$TREN	1:1:1	100:1:1
		100:2:1
PMDETA	1:1.2:1	100:1:1

3.4.1.1 Concurrent RAFT-ARGET ATRP
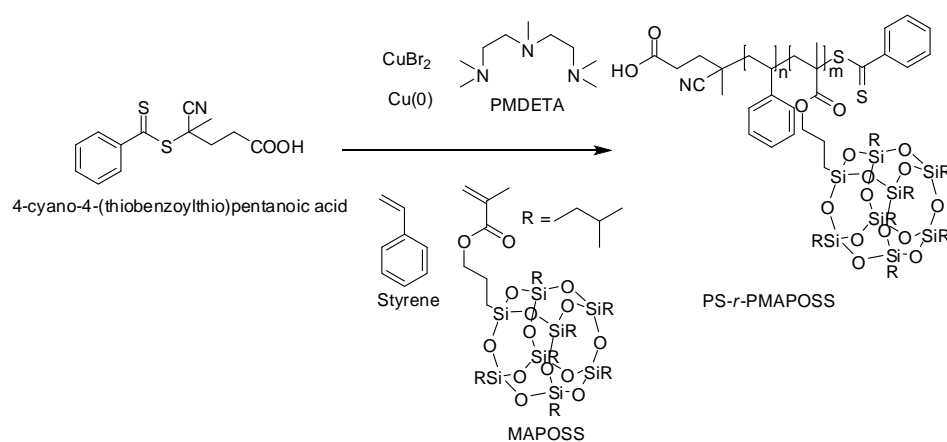
CuBr$_2$ (2 mg, 0.008 mmol), PMDETA (26 μL, 0.12 mmol), CVADTB (12 mg, 0.043 mmol) (molar ratio of 1:140:5), copper wire (4.8 g, 0.076 mol) and various amount of styrene and MAPOSS (**Table 3.3**) were added into a 25 mL scintillation vial, which was then sealed with rubber septum. After being purged with nitrogen gas for 15 minutes, the reaction was carried out under nitrogen atmosphere at 90∘C for 24 hours.

Table 3.3 Mass ratio and molar ratio of styrene and MAPOSS used in the synthesis of PS-*r*-MAPOSS with target Mn of 130 kDa

Sty:MAPOSS (by mass)	Sty:MAPOSS:CVADTB (by mol)
19:1	1186:7:1
9:1	1123:14:1
3:1	936:34:1

3.4.2 Block Copolymers (PS-*b*-PMAPOSS, PS-*b*-(PMMA-*r*-PMAPOSS), PS-*b*-(PS-*r*-PMAPOSS))
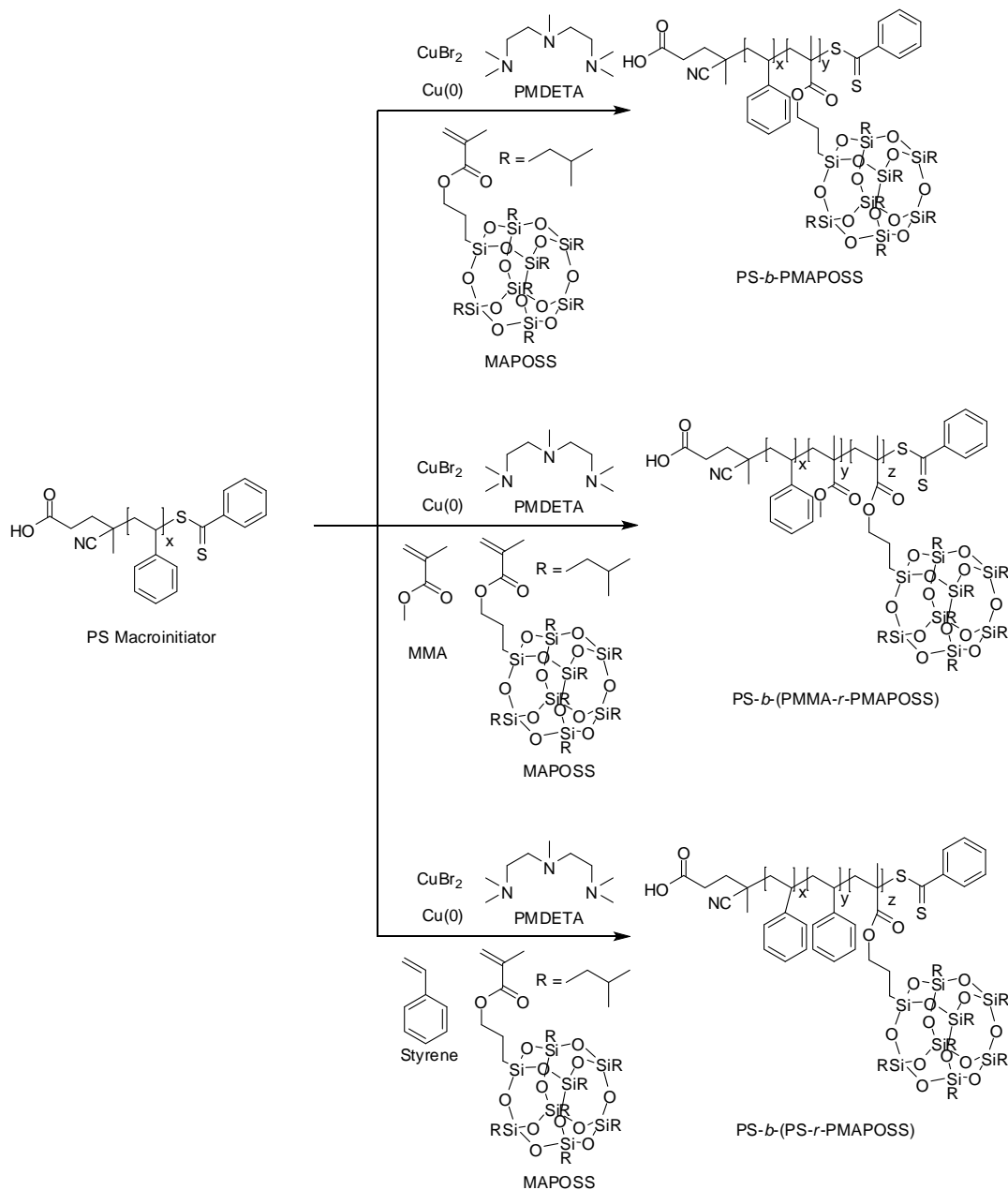
Block copolymer syntheses were separated into 2 parts. First, PS macroinitiator was synthesized using concurrent RAFT-ARGET ATRP method as described in section 3.3.4. PS macroinitiator was then added into a 10 mL vial, followed by CuBr$_2$ (2 mg, 0.008 mmol), PMDETA (26 µL, 0.12 mmol) (molar ratio of CuBr$_2$:PMDETA:PS macroinitiator 1:140:5), copper wire (4.8 g, 0.076 mol), and

designated amount of monomers (**Table 3.3**). The vial was then sealed with rubber septum. After being purged with nitrogen gas for 15 minutes, the reaction was carried out under nitrogen atmosphere at 90∘C for 24 hours.

Table 3.4 Molar ratio of monomers used in the synthesis of block copolymers

Block type	Target M_n (kDa)	M_n of PS macroinitiator (kDa)	Monomer ratio in second block (by mass)	Monomer:PS macrointiator in second block (by mol)
PS-*b*-PMAPOSS	114	96.4	Pure MAPOSS	19:1
PS-*b*-(PMMA-PMAPOSS)	130	62.9	MMA:MAPOSS = 1:1	MMA:MAPOSS: initiator = 335:36:1
PS-*b*-(PS-PMAPOSS)	130	62.9	Styrene:MAPOSS = 1:1	styrene:MAPOSS: initiator = 322:36:1

3.5 Purification of the Synthesized (Co)polymers

Synthesized (co)polymers were first dissolved in THF, and then passed through basic alumina column to remove catalysts. Polymer solution was then precipitated in rigorously stirred ethanol. The products were then dried under vacuum overnight.

3.6 Electrospinning

The synthesized (co)polymers were dissolved in a mixed solvent of tetrahydrofuran (THF) and dimethylformamide (DMF) having various volume ratio to prepare 20% w/v polymer solutions. Each of the as-prepared solution was loaded into a syringe connected to an equipment setting as shown in **Figure 3.1**. Polymer solution was electrospun onto aluminum foil with 20 kV electric field, 15 cm collection distance, and flow rate of 4.5 mL/h for PS and 6.5-8.5 mL/h for PS-*co*-PMAPOSS. Electrospun fiber mats were left to dry for 24 hours prior to characterization.
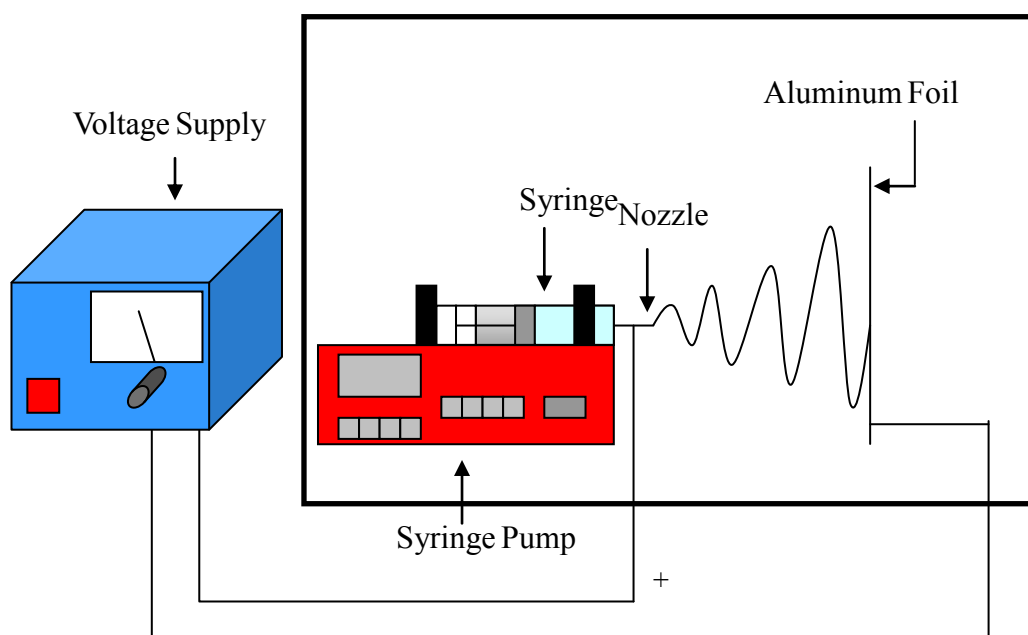
Figure 3.1 Set up for electrospinning

CHAPTER IV

RESULTS AND DISCUSSION

This chapter is divided into 2 parts. The first part focuses on the (co)polymer synthesis and characterization. The second part is dedicated to investigation on electrospinning of the synthesized (co)polymers and characterization of the obtained fiber mats.

4.1 Syntheses of PS and PS-*co*-PMAPOSS

4.1.1 Effect of Catalyst and Polymerization Method

Polymerization of styrene can be confirmed by ^{1}H-NMR analysis. As shown in **Figure 4.1**, the decrease in intensity of peaks at 6.7, 5.8 and 5.3 ppm, assigned to vinyl protons of styrene (b, c, d, respectively in **Figure 4.1A**) apparently disappeared after polymerization and purification (**Figure 4.1C**) indicating that styrene was consumed upon polymerization and transformed into polystyrene (PS) of which the signals of methylene protons of PS backbone can be seen at 1.2-2.0 ppm (b' and c' in **Figure 4.1B and C**). The signals of aromatic protons of styrene at 7.2-7.5 ppm were shifted upfield to 6.3-7.2 ppm when it was polymerized into PS. The sharp peaks appear in a range of 1.0-2.5 ppm are remaining solvent used for purification (THF or ethanol). It should be noted that such peak intensity became lower after repetitive purification. It should also emphasized thatthe shape of peak b' and c', which corresponded with PS chain backbone, depended upon tacticity of the polymer [31].
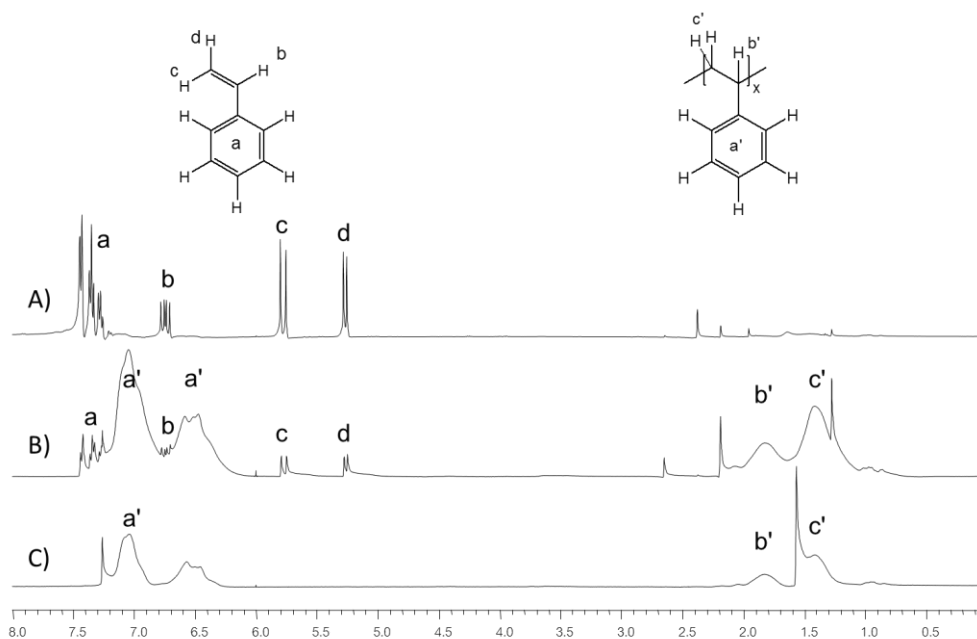
Figure 4.1 ^{1}H NMR spectra of styrene (A) and PS before (B) and after (C) purification.

From **Table 4.1**, preliminary investigation on polymerization of styrene (Sty) by ATRP method using Me$_6$TREN was proven to be ineffective, as polydispersity index (PDI) at low monomer to initiator ratio (Sty:EBiB ratio = 100:1) was 1.43, signifying poor control over polymerization, and polymerization did not occur at all even at extended duration at high Sty:EBiB ratio (500:1). This could be the result of poor solubility of Cu(II)-Me$_6$TREN complex in styrene that shift the equilibrium to the right, resulting in too much of radical species present. By using PMDETA as ligand, of which Cu(II) complex had better solubility, lower PDI (1.08) was achieved but reaction seemed to proceed at a slower rate, as indicated by the lower molecular weight of the obtained PS.

Table 4.1 Molecular weight and PDI of PS synthesized via ATRP as a function of monomer feed ratio and ligand.

Sty:EBiB	Ligand	Reaction Time (h)	Target M_n^a (kDa)	M_n (kDa)	M_w (kDa)	PDI
100:1	Me$_6$TREN	24	10.4	8.7	12.5	1.43
200:1	Me$_6$TREN	24	20.8	20.1	22.3	1.12
500:1	Me$_6$TREN	72	52.0	-	-	-
100:1	PMDETA	24	10.4	7.9	8.5	1.08
500:1	PMDETA	48	52.0	27.2	29.5	1.08

^{a}Target M_n = Sty/EBiB x 104.15

As for PS-*r*-PMAPOSS, the presence of MAPOSS unit can be verified by signals of methyl and methylene protons in isopropyl groups of MAPOSS at 0.9-1.0 ppm (c' in **Figure 4.2B-C**) and 0.6 ppm (d' in **Figure 4.2B-C**), respectively. The signal of methylene protons in the copolymer backbone was found as a broad peak in 1.2 - 2.0 ppm region (b' in **Figure 4.2B-C**). According to the results shown in **Table 4.2**, PMDETA was proven to be a better ligand than Me$_6$TREN considering the ability to attain PDI as low as 1.07. This is similar to what has been observed for PS synthesis described earlier.
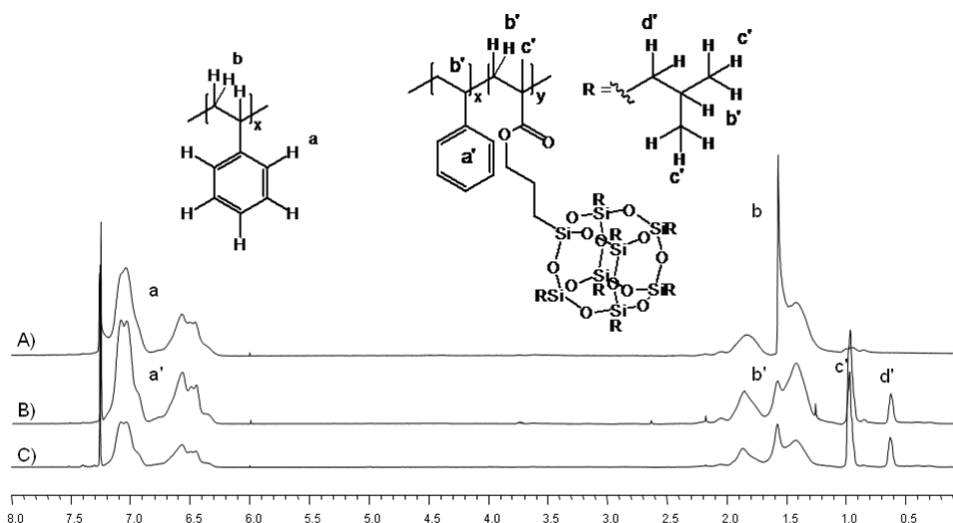
Figure 4.2 ^{1}H NMR spectra of PS (A) and PS-*r*-PMAPOSS with MAPOSS:Sty mol feed ratio of 1:100 (B) and 1:50 (C).

Table 4.2 Molecular weight and PDI of PS-*r*-PMAPOSS synthesized via ATRP as a function of monomer feed ratio and ligand.

Sty:MAPOSS: EBiB	Ligand	Reaction Time (h)	M_n (kDa)	M_w (kDa)	PDI
100:1:1	Me$_6$TREN	9	12.7	16.4	1.29
100:2:1	Me$_6$TREN	9	18.5	24.0	1.29
100:1:1	PMDETA	9	16.5	17.7	1.07

Comparative investigation on the effectiveness of polymerization method used for the preparation of PS was performed using Sty:EBiB of 500:1. The results outlined in **Table 4.3** suggested that ATRP was the least efficient method as shown through its slowest rate of polymerization. As long as 72 h of polymerization was necessary to get PS with M_n of 42.3 kDa, considering that the target M_n of 50 kDa was expected. A very high PDI of 2.33 obviously indicated that the polymerization was uncontrolled. Due to unavoidable accumulation of Cu(II) as the polymerization proceeded due to side reaction and trace oxygen, ATRP was thus not a suitable method for the synthesis of polymer with high molecular weight of which long

reaction time is usually required. On the other hand, ARGET ATRP gave the highest polymerization rate (M_n of 66.5 kDa was achieved in 24 h). This could be the result of added reducing agent (copper wire), which can reduce the amount of Cu(II) in the equilibrium, resulting in less side reaction and increase in polymerization kinetic. The obtained PDI of 1.54, however, suggested that the polymerization by ARGET ATRP was still not well controlled. Concurrent RAFT-ARGET ATRP, with polymerization under control of 2 equilibriums (one for RAFT, the other for ARGET ATRP), provided a copolymer product with a better control over M_n and PDI. Thus, concurrent RAFT-ARGET ATRP was chosen as the method to be used for polymerization of high molecular weight PS and copolymers.

Table 4.3 Molecular weight and PDI of PS synthesized by various living polymerization methods.

Method	Sty:EBiB	Reaction Time (h)	M_n (kDa)	M_w (kDa)	PDI
ATRP		72	42.3	98.6	2.33
ARGET ATRP	500:1		66.5	102.7	1.54
RAFT		24	56.2	69.9	1.25
Concurrent RAFT - ARGET ATRP			57.1	66.3	1.16

4.1.2 Synthesis of (Co)polymers by Concurrent RAFT - ARGET ATRP

For polymer to be able to form fibers by itself via electrospinning, molecular weight of the polymer has to be high enough to provide sufficient chain entanglement. Therefore, this research aimed to synthesize PS and PS-co-PMAPOSS with molecular weight higher than 100 kDa to ensure electrospinnability. As shown in **Table 4.4**, poor control over molecular weight and PDI was achieved when Sty:EBiB exceeded 500:1 (target M_n of 50 kDa). Attempt to improve polymerization

efficiency by an addition of reducing agent, copper wire, was not successful as can be realized from the polymerization solution being not viscous together with the fact that GPC trace was not found (the M_n and M_w in last entry in **Table 4.4** were not available) implying that PS did not form. Because the mechanism of polymerization was governed by equilibrium, too high concentration of Cu(0) could drive the equilibrium to the right, resulting in high content of radical species.. In principle, the higher radical concentration promotes termination. For this reason, the extension of polymer chain by propagation was no longer the dominating process. Under such circumstance, the polymer can hardly form.

Table 4.4 Molecular weight and PDI of PS synthesized via concurrent RAFT-ARGET ATRP

Sty : CVADTB	Copper wire (g)	M_n (kDa)	M_w (kDa)	PDI
500:1		57.1	66.3	1.16
1000:1	0.48	94.7	131.1	1.38
1300:1		158.9	199.4	1.25
1000:1	0.96	n/a	n/a	n/a

Syntheses of PS-co-PMAPOSS, however, required higher amount of copper than that used in the synthesis of PS. By using 0.48 g of copper wire, polymerization did not occur in spite of the extended reaction for up to 72 hours. The successful synthesis of PS-*r*-PMAPOSS of which M_n (131.7 kDa) can reach the expected target (130 kDa) can be accomplished by using 0.96 g of copper wire.

GPC traces shown in **Figure 4.3** implied that the copolymerization of Sty and MAPOSS yielded PS-*r*-PMAPOSS with multiple molecular weight range.
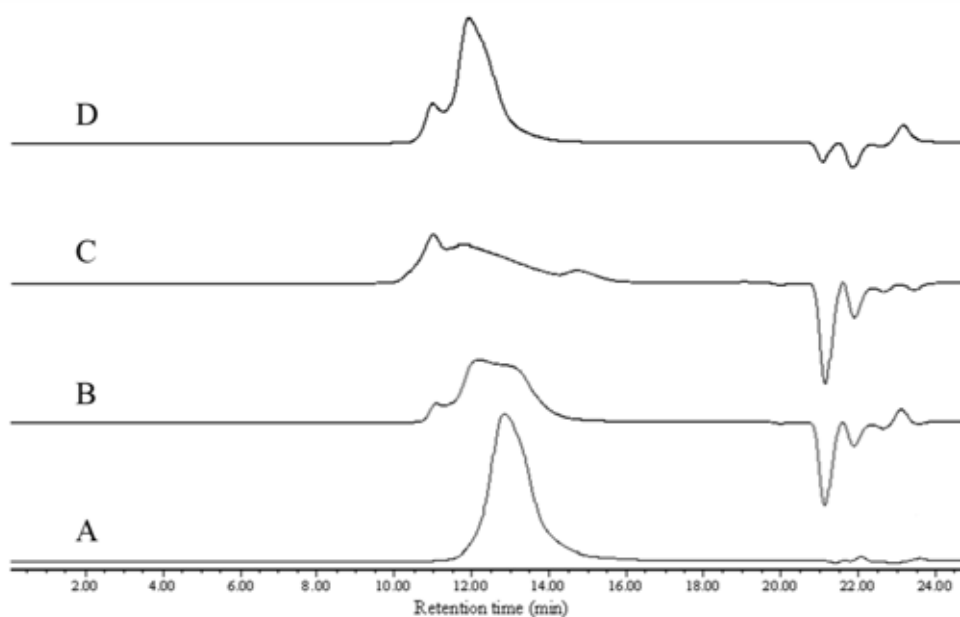
Figure 4.3 GPC traces of PS (A) and PS-*r*-PMAPOSS with MAPOSS:Sty feed ratio of 5:95 (B), 10:90 (C) and 25:75 (D).

Polymerization of styrene and MAPOSS can be confirmed by ^{1}H-NMR analysis. As can be seen from **Figure 4.4**, the increase in intensity of peaks at 0.9-1.0, assigned to methyl protons on isopropyl groups of MAPOSS, and at 0.6 ppm, assigned to methylene protons on isopropyl groups of MAPOSS (c' and d', respectively in **Figure 4.4A, B, C**) as a function of MAPOSS content suggested that the MAPOSS composition in the copolymer can be controlled by the MAPOSS content in the feed. There were also no peaks appearing in the range of 5.5-6.0 ppm that can be assigned to methylene protons of monomers meaning that all unreacted residual monomers were removed after purification and separation.
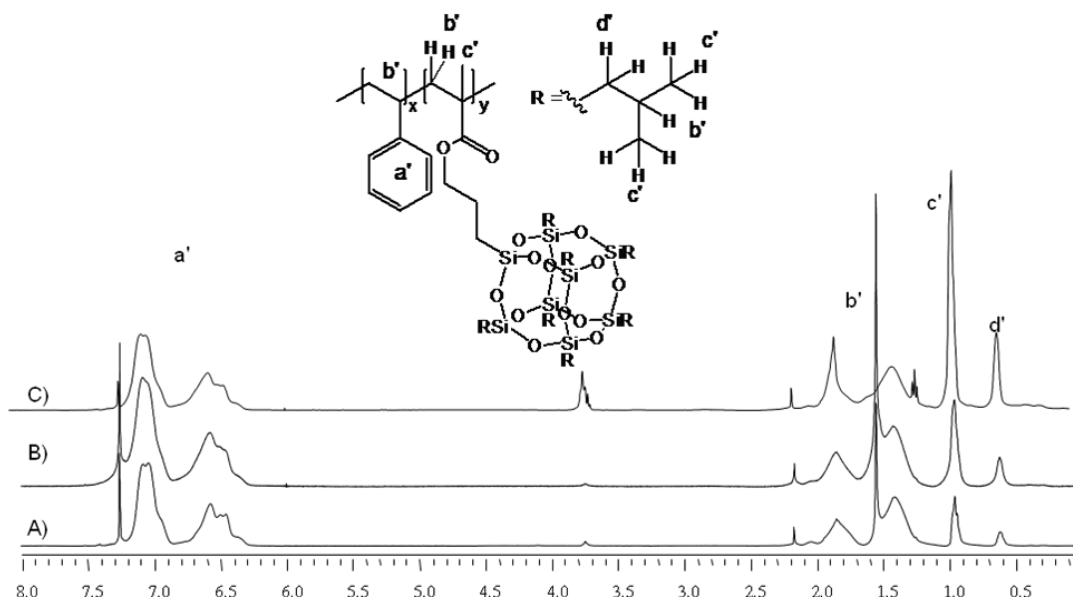
Figure 4.4 ^{1}H NMR spectra of PS-*r*-PMAPOSS with MAPOSS: Sty feed ratio of 5:95 (A), 10:90 (B), and 25:75 (C).

The content of MAPOSS (%MAPOSS) or MAPOSS composition in the copolymer can be determined by two methods; one by ^{1}H NMR and the other by TGA data. By using ^{1}H NMR data, the %MAPOSS by mole and weight can be calculated using equation 4.1 and 4.2, respectively

$$\%MAPOSS\ (mol) = \frac{(D/14)}{(D/14)+(A/5)}$$

(4.1)

$$\%MAPOSS\ (mass) = \frac{(943.64D/14)}{(943.64D/14)+(104.15A/5)}$$

(4.2)

Where D is the integration of peak d' assigned to methylene protons in isopropyl group of MAPOSS, in which each unit has 14 and A is the integration of peak a' assigned to aromatic protons in phenyl group of styrene, in which each unit has 5.

TGA thermograms, which are the thermal decomposition profile of PS and all random (co)polymers, are illustrated in **Figure 4.5**. Apparently, the incorporation of a certain percentage of PMAPOSS (14 and 36%) increased the copolymer thermal stability as can be realized from the elevated decomposition temperature (See data in **Table 4.5**). As anticipated, %Ash correspondingly increased as a function of PMAPOSS content.
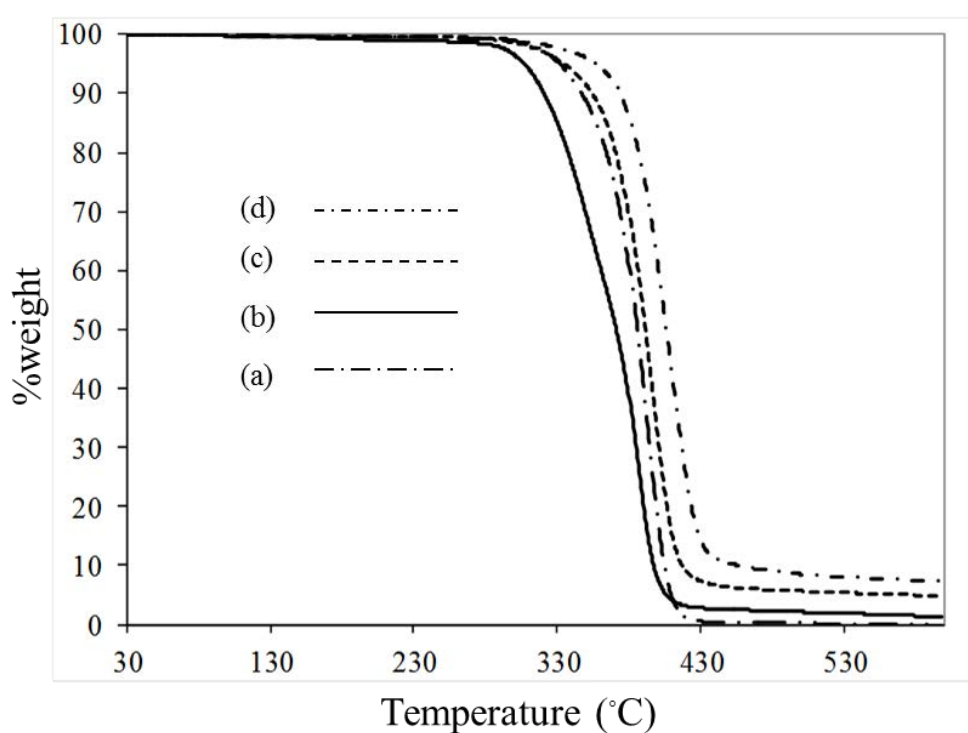
Figure 4.5 TGA thermograms of PS (a) and PS-*r*-PMAPOSS with MAPOSS:styrene feed ratio of 5:95 (b), 10:90 (c) and 25:75 (d).

Table 4.5 Decomposition temperature, %Ash and %weight loss of PS and random copolymers analyzed with STARe SW program version 9.30

Polymer	Decomposition Temperature[a] (°C)	%Ash[b]	%weight loss[c]
PS	281	0.073	99.927
PS-*r*-PMAPOSS 9%	281	1.248	98.752
PS-*r*-PMAPOSS 14%	284	4.882	95.118
PS-*r*-PMAPOSS 36%	295	7.436	92.564

[a]the decomposition temperature is identified as the temperature at which the weight loss begins
[b]%Ash is identified as the weight left after the decomposition process.
[c]%weight loss is equal to 100 - %Ash

From the data shown in **Table 4.5**, %MAPOSS can be calculated using the following equation:

$$\%\text{MAPOSS (mass)} = \frac{(943.64 \text{ x } \%Ash/14)}{(943.64 \text{ x } \%Ash/14)+(\%weight\ loss)} \text{ x } 100$$

(4.3)

Where %Ash and %weight loss were obtained from the final %weight and the difference between the final %weight and beginning %weight (100%), respectively (reported in **Table 4.5**). The numbers of 943.64, 104.15, and 480.32 appeared in the equations 4.2-4.3 are molecular weight of MAPOSS, styrene, and 8 moiety of silica, respectively. Weight loss due to decomposition of MAPOSS moiety was negligible when compared with that of PS moiety.

The %MAPOSS by mass calculated from NMR and TGA data and molecular weight of the copolymers are displayed together in **Table 4.6**. Molecular weight of

the obtained copolymers closely resembled that of the target molecular weight of 130 kDa. The composition of MAPOSS in the copolymer calculated by both methods progressively increased with the MAPOSS composition in the feed. The compositions calculated from NMR data seemed to be greater than the anticipated values implying the MAPOSS is more reactive towards copolymerization than Sty. In contrast, the composition calculated from TGA data was underestimated when compared with the MAPOSS in the feed. This may be explained by a possible sublimation of MAPOSS free from the copolymer via depolymerization that may occur simultaneously with degradation of organic residues. As a consequence, the remaining silica content was then lower than anticipated due to the loss of MAPOSS during the thermal degradation.

Table 4.6 Molecular weight and composition of PS-*r*-PMAPOSS as a function of monomer mol feed ratio.

Sty:MAPOSS: CVADTB	M_n (kDa)	%MAPOSS by mass		
		in feed	obtained by NMR	obtained by TGA
1251:7:1	111.1	5	9	2
1185:14:1	129.6	10	14	10
987:36:1	131.7	25	36	15

XRD spectra of MAPOSS, PS, and random copolymer are shown in **Figure 4.6**. Lack of sharp peak in the spectrum of PS (**Figure 4.6B**) indicated that the majority of PS is amorphous. At low %MAPOSS (5%in feed), the spectral intensity (**Figure 4.6C**) dropped significantly implying that the addition of small amount of MAPOSS disrupted the packing of PS chains. At greater %MAPOSS (10, 25% in feed), the peak intensity became comparable to that of PS which is still dominated by amorphous phase.
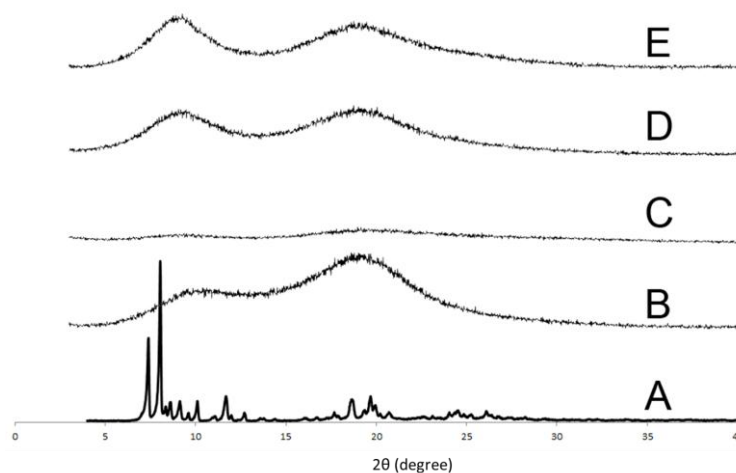
Figure 4.6 XRD spectra of MAPOSS(A), PS (B) and PS-*r*-PMAPOSS with MAPOSS:Sty feed ratio of 5:95 (C), 10:90 (D), and 25:75 (E).

As for block copolymer, the content of MAPOSS (%MAPOSS) or MAPOSS composition in the copolymer can be determined by ^{1}H NMR (**Figure 4.7**). For PS-*b*-PMAPOSS and PS-*b*-(PS-PMAPOSS), the %MAPOSS by mole and weight can be calculated using the same equations as mentioned above (4.1 and 4.2). As for PS-*b*-(PMMA-PMAPOSS), the %MAPOSS by mole and weight can be calculated by the following equations:

$$\%\text{MAPOSS (mol)} = \frac{(C/14)}{(C/14)+(A/5)+((B/3)-3(C/14))} \tag{4.4}$$

$$\%\text{MAPOSS (mass)} = \frac{(943.64D/14)}{(943.64D/14)+(104.15A/5)+100.12((B/3)-3(C/14))} \tag{4.5}$$

Where C is the integration of peak c assigned to methylene protons in isopropyl group of MAPOSS, in which each unit has 14, A is the integration of peak a assigned to aromatic protons in phenyl group of styrene, in which each unit has 5,

and B is the integration of peak b assigned to methyl protons in isopropyl group of MAPOSS and methacrylate unit, in which each unit has 3
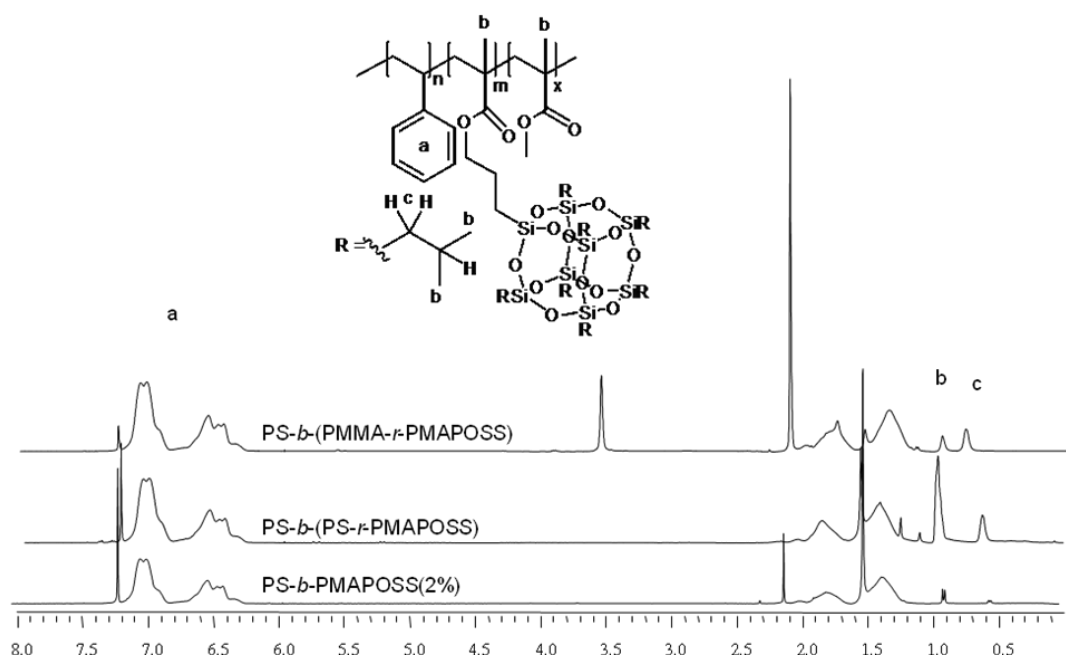
Figure 4.7 ^{1}H NMR spectra of PS-*b*-PMAPOSS , PS-b-(PS-r-PMAPOSS) and PS-b-(PMMA-*r*-PMAPOSS).

Early attempt to synthesize PS-*b*-PMAPOSS from PS macroinitiator having M_n of 96.4 kDa by direct polymerization of MAPOSS was unsuccessful. It was found that very low content of MAPOSS was incorporated into the copolymer despite a significantly high molecular weight of the obtained product (122.2 kDa). This may be explained as a result of steric hindrance inherited with the bulky POSS group. In later attempt, Sty or methyl methacrylate (MMA) was mixed with MAPOSS in the syntheses of the second block in order to overcome the problem due to steric hindrance. As shown in **Table 4.7**, an increase of %MAPOSS was noticeable (%MAPOSS by mass = 16% in the case of PS-*b*-(PMMA-*r*-PMAPOSS) and 20% in the case of PS-*b*-(PS-*r*-PMAPOSS)) whereas the molecular weight of the synthesized copolymer (81.2 kDa) was still lower than expected (130 kDa).

Table 4.7 Molecular weight and composition of block copolymers as a function of monomer feed ratio.

Block type	Target M_n (kDa)	M_n of PS macroinitiator (kDa)	Monomer ratio in second block (by mass)	M_n (kDa)	%MAPOSS by mass (NMR)
PS-*b*-PMAPOSS	114	96.4	Pure MAPOSS	122.2	2
PS-*b*-(PMMA-*r*-PMAPOSS)	130	62.9	1:1 (MMA:MAPOSS)	81.2	16
PS-*b*-(PS-*r*-PMAPOSS)	130	62.9	1:1 (Sty:MAPOSS)	n/a	20

4.~~3~~ 2 Electrospinning of (Co)polymers

4.~~3~~2.1 Effect of Solvent on Electrospun PS Fibers

Previously, it has been shown in literatures that solvent has a strong impact on morphological features of electrospun fiber [17]. In this research, both single solvent (THF or DMF) and mixed solvent of THF and DMF having various volume ratios were tested as media to solubilize the (co)polymers for electrospinning. The results illustrated in **Figure 4.8a** suggested that THF was not a good solvent for PS. The electrospun PS were mostly in the form of large beads with very few fibers were formed. This might be the result of PS solution in THF having less surface tension than that in DMF [17]. Fast evaporation of THF also promoted the bead formation. DMF alone could yield bead-free fibers although fiber diameter distribution was relatively large (see number written underneath the micrographs in **Figure 4.8d**). This may be described by the slow evaporation of DMF being an obstacle for uniform fiber formation. Mixed solvent of THF and DMF of both volume ratios (2:1 and 1:2), on the other hand, resulted in fibers with better consistency in fiber diameter (**Figure 4.8b-c**).

Beads — 2.4±0.4 μm — 2.7±0.4 μm — 3.3±1.4 μm
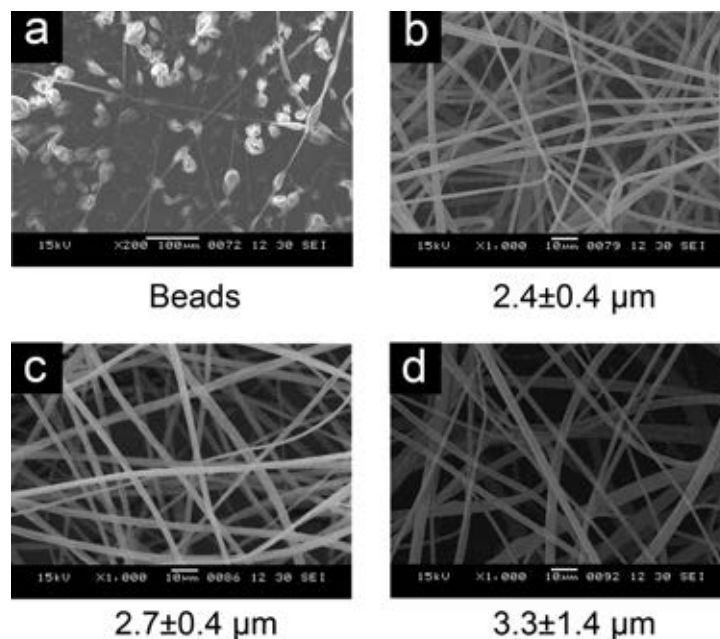
Figure 4.8 SEM micrographs of electrospun fibers obtained from PS solution in THF (a), mixed solvent of THF:DMF with the volume ratio of 2:1 (b) and 1:2 (c), and DMF (d). Below each micrograph is the average diameter of the corresponding electrospun fibers.

4.~~3~~2.2 Effect of Solvent and Copolymer Composition on Electrospun PS-*co*-PMAPOSS Fibers

Both random and block copolymer fiber mats were fabricated using similar setting used for fabricating PS fiber mats. Relatively uniform fibers were obtained by electrospinning PS-*r*-PMAPOSS (%MAPOSS =36%) dissolved in THF (**Figure 4.9a**). The random copolymer was not soluble but only swelled in DMF. It was soluble only when THF was incorporated with a mixed volume ratio of at least 1:2. Nevertheless, the PS-*r*-PMAPOSS fibers electrospun from the mixed solvents were less uniform with a broader distribution of fiber diameter as the DMF content increased, as depicted in **Figure 4.9b-c**,

| 6.4±1.5 µm | 7.7±1.7 µm | 7.6±3.6 µm |
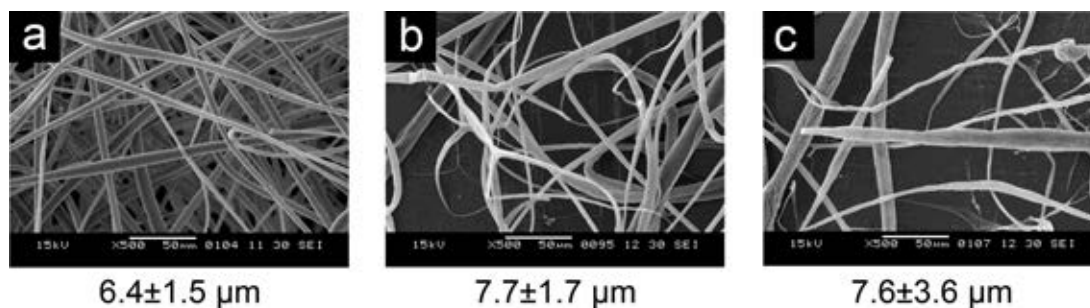
Figure 4.9 SEM micrographs of electrospun fibers obtained from PS-*r*-PMAPOSS (%MAPOSS = 36) solution in THF (a) and mixed solvent of THF:DMF with the volume ratio of 2:1 (b) and 1:2 (c). Below each micrograph is the average diameter of the corresponding electrospun fibers.

Additionally, the fiber surface and inner morphology were also greatly affected by solvent mixture ratio as can be viewed from micrographs shown in **Figure 4.10**. Using THF alone, the obtained fibers had smooth surface and was dense, with no observable porosity. Addition of DMF, however, caused the as-spun fiber surface to be rougher having "wood-like" longitudinal grooved feature that was more pronounced at higher DMF content. The cross-sectional images shown in **Figure 4.10d-f** indicated that the fibers fabricated from the mixed solvent were very porous. Relatively hollow fibers with large "cheese-like" pores and fibers with a lot of small "sponge-like" pores were formed when the copolymer was electrospun from the solution of mixed solvent with the volume ratio (THF:DMF) of 2:1 and 1:2, respectively.
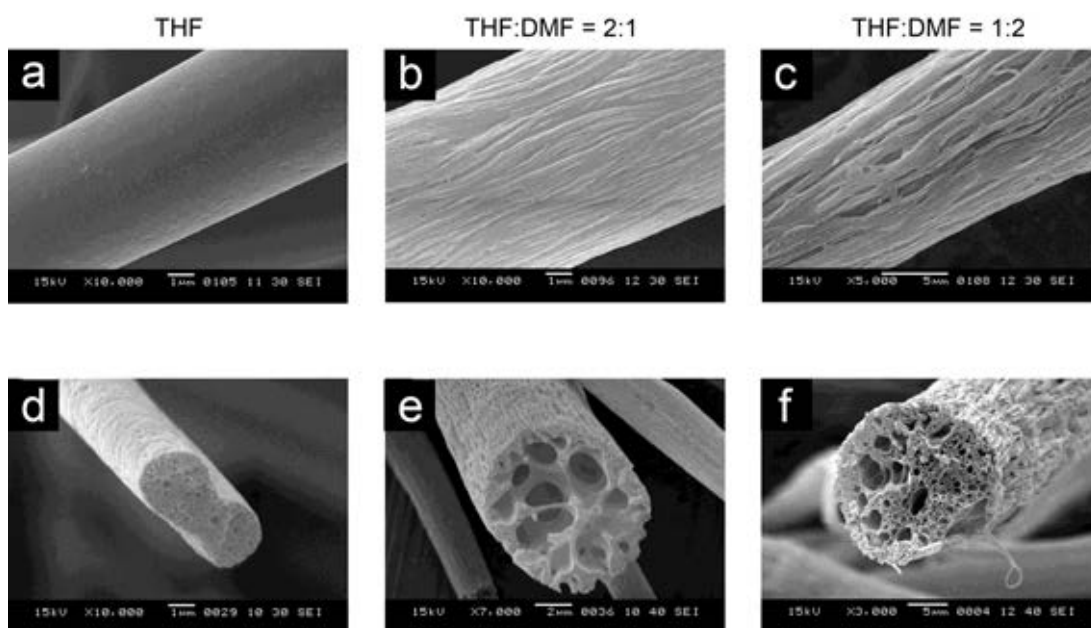
Figure 4.10 SEM micrographs demonstrating surface texture (a-c) and inner porosity (d-f) of electrospun fibers obtained from PS-*r*-PMAPOSS (%MAPOSS = 36) solution in THF (a,d) and mixed solvent of THF:DMF with the volume ratio of 2:1 (b,e) and 1:2 (c,f).

The amount of MAPOSS in the copolymer also had a strong impact on the fiber size and morphology (**Figures 4.11-4.12**). At low %MAPOSS, the fiber diameters (2.9 µm and 2.7 µm for solvent ratio of THF:DMF = 2:1 and 1:2, respectively) were comparable to that of the PS homopolymer (2.4 µm and 2.7 µm for solvent ratio of THF:DMF = 2:1 and 1:2, respectively). Increasing in the MAPOSS content gave fibers with larger diameter. The average fiber diameter was 2.8, 6.1, and 7.2 µm for the electrospun PS-*r*-PMAPOSS having %MAPOSS of 9, 14, and 36, respectively. Porosity of the fiber also followed the same trend by becoming more pronounced at higher %MAPOSS.
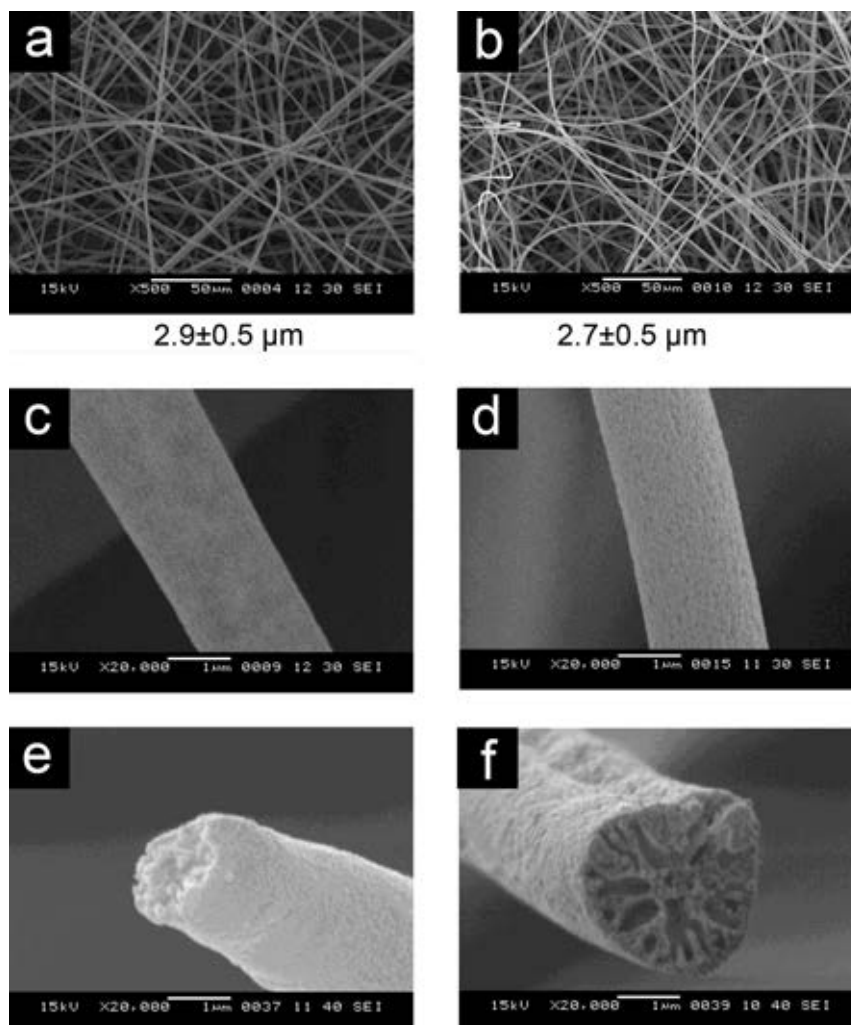
Figure 4.11 SEM micrographs demonstrating overall morphology (a,b), surface texture (c,d), and inner porosity (e,f) of electrospun fibers obtained from PS-*r*-PMAPOSS (%MAPOSS = 9%) solution in mixed solvent of THF:DMF with the volume ratio of 2:1 (a,c,e) and 1:2 (b,d,f). Below the micrographs a and b re the average diameter of the corresponding electrospun fibers.

Figure 4.12 SEM micrographs demonstrating overall morphology (a,b), surface texture (c,d), and inner porosity (e,f) of electrospun fibers obtained from PS-*r*-PMAPOSS (%MAPOSS = 14%) solution in mixed solvent of THF:DMF with the volume ratio of 2:1 (a,c,e) and 1:2 (b,d,f). Below the micrographs a and b are the average diameter of the corresponding electrospun fibers.

In the case of block copolymer, all electrospun fibers were fabricated from mixed solvent with THF:DMF volume ratio of 2:1. According to **Figure 4.13**, all block copolymers gave fibers with relatively smaller diameter than that of the PS homopolymer and the random copolymers having high %MAPOSS content (14 and 36%). This could be the result of lower chain entanglement because the block copolymers possessed relatively lower molecular weight than the random ones.

Apparently, PS-*b*-(PMMA-*r*-PMAPOSS) gave fibers with a broader diameter distribution than other two systems (PS-*b*-PMAPOSS and PS-*b*-(PS-*r*-PMAPOSS). Its surface roughness seemed to be random, unlike other two systems of which roughness had longitudinal grooved pattern. Having 3 types of polymeric units with different polarity (PS, PMMA, and PMAPOSS) in the structure of PS-*b*-(PMMA-*r*-PMAPOSS) might add complication to fiber formation, resulted in both poor fiber diameter consistency and random nature of roughness.
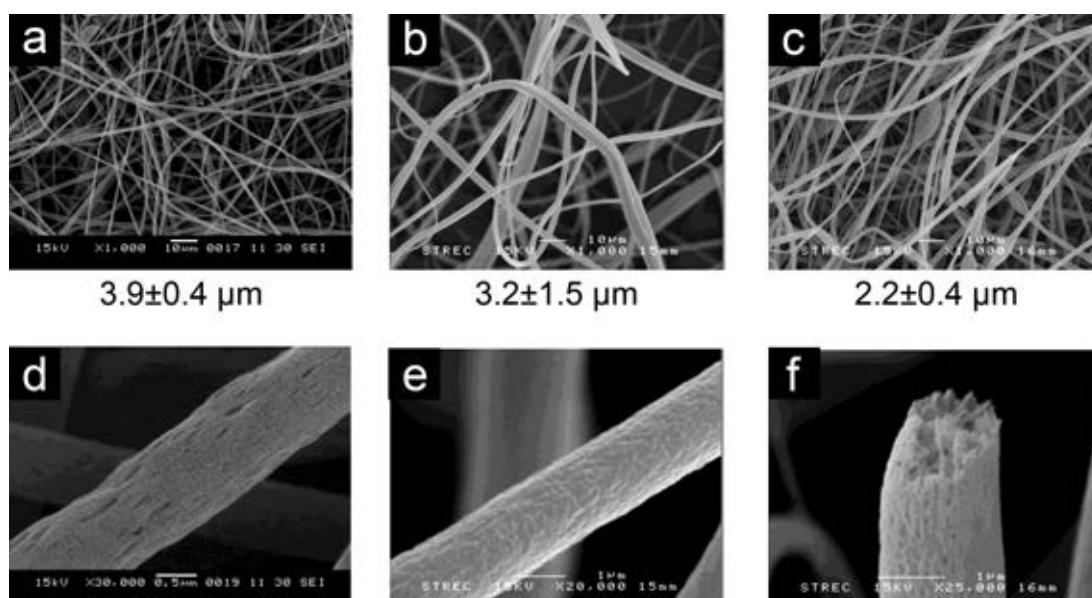
Figure 4.13 SEM micrographs demonstrating overall morphology (a-c), surface texture (d-f) of electrospun fibers obtained from PS-*b*-PMAPOSS (a), PS-*b*-(PMMA-*r*-PMAPOSS) (b) and PS-*b*-(PS-*r*-PMAPOSS) (c) solution in mixed solvent of THF:DMF with the volume ratio of 2:1. Below the micrographs a-c are the average diameters of the corresponding electrospun fibers.

To further understand the mechanism of fiber formation, electrospun fiber mats were further investigated by SEM/EDS technique. As seen in **Table 4.7**, the elemental composition of PS-*r*-PMAPOSS fiber surface changed according to the solvent used. With THF, which was good solvent for both PS and PS-*r*-PMAPOSS, elemental composition of fiber almost matched the theoretical estimation calculated

from that of the bulk composition, The addition of DMF in solvent, which was poor solvent for PS-*r*-PMAPOSS, caused a decrease in silicon content, which corresponded to MAPOSS moiety. XRD spectra of electrospun fiber (**Figure 4.14**) indicated that the crystallinity of PS fibers was not affected by the solvent used for electrospinning, In contrast, the phase morphology of electrospun PS-*r*-PMAPOSS fibers was influenced by the solvent suggesting a possible chain re-orientation upon solvent change. While both PS and PMAPOSS phase were both well dispersed when THF was used as solvent, PS phase seemed to be more abundant at the surface than PMAPOSS phase when DMF was added. This implied that the variation in PS-*co*-PMAPOSS fiber morphology (formation of pore and roughness) was probably driven by DMF-induced phase separation of which proposed mechanism is schematically displayed in **Figure 4.15**. When THF was used as solvent in electrospinning, good dispersion of both PS and PMAPOSS phase led to formation of fiber with uniform surface and narrow fiber diameter distribution. Mixed solvent of THF and DMF, on the contrary, forced the phase separation, with PMAPOSS rearranged to be further from the surface while PS rearranged to be closer to the surface, leading to formation of "bubble-like" comformation. Solvent evaporation caused inner morphology of fiber to be porous, while stretching and whipping of fiber during electrospinning broke and stretched "bubble-like" comformation of polymer solution, resulting in "wood-like" longitudinal grooves on the surface.

Table 4.8 Elemental composition obtained by SEM/EDS of random copolymers.

THF:DMF	Elemental Composition (%)		
	C	O	Si
Theoretical	88.16	7.53	4.30
3:0	87.78	7.60	4.62
2:1	85.15	11.08	3.77
1:2	84.73	12.20	3.06
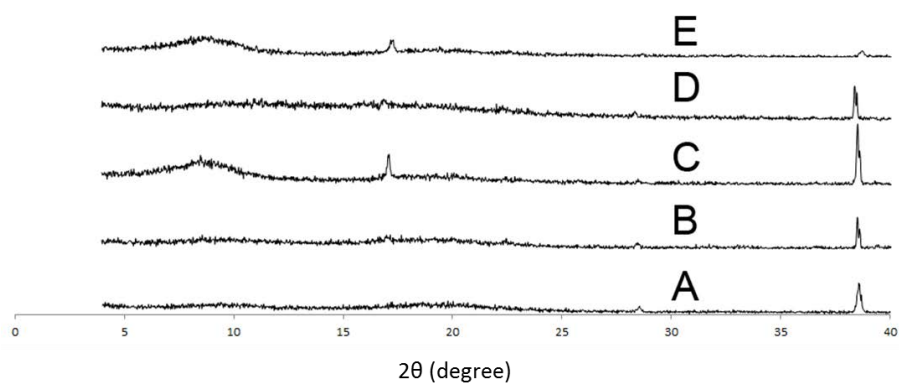
Figure 4.14 XRD spectra of electrospun fibers obtained from PS solution in mixed solvent of THF:DMF with the volume ratio of 2:1 (a) and 1:2 (b) and PS-*r*-PMAPOSS (%MAPOSS = 36) solution in THF (c) and mixed solvent of THF:DMF with the volume ratio of 2:1 (d) and 1:2 (e).
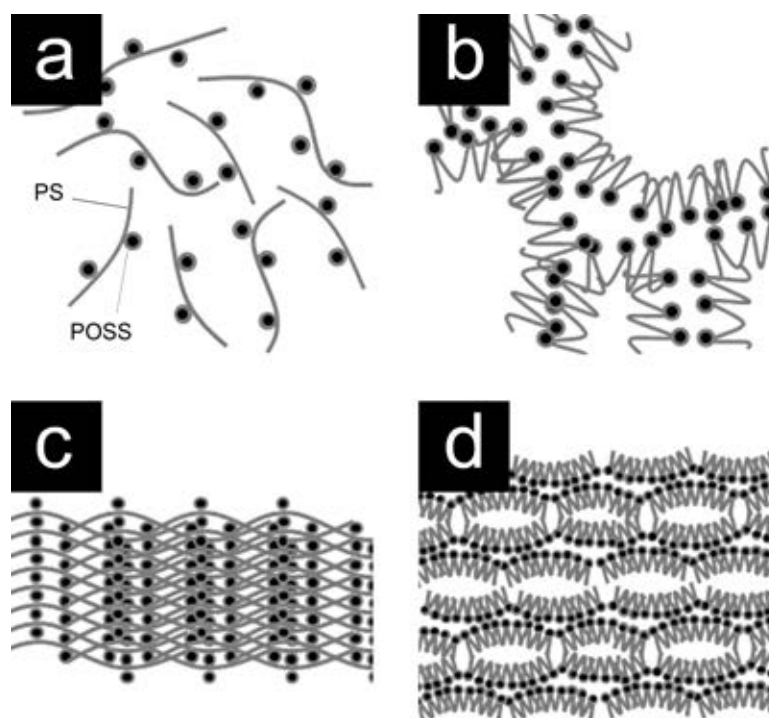
Figure 4.15 Schematic illustration of proposed mechanism of formation of pores and roughness in PS-*co*-PMAPOSS fiber: the PS-*co*-PMAPOSS in (a) THF solution and (b) mixed solvent of THF and DMF and as-spun fiber electrospun from (c) THF solution and (d) mixed solvent of THF and DMF-.

The additional roughness and porosity introduced to the fibers would increase the surface roughness of the fiber mats. Together with the fact that the copolymers are hydrophobic, the electrospun fiber mats may be useful for the development a new class of superhydrophobic POSS-based material. Nevertheless, several characteristics of the fibers must be improved such as fiber diameter, diameter consistency.

CHAPTER V

CONCLUSION AND SUGGESTIONS

Preliminary investigation on polymerization of styrene (Sty) by ATRP method using Me_6TREN and PMDETA as ligand showed that Me_6TREN was not an effective ligand, which could be the result of poor solubility of Cu(II)-Me_6TREN complex in styrene. PMDETA, of which Cu(II) complex had better solubility, the polymer with lower PDI (1.08) was achieved but reaction seemed to proceed at a slower rate.

Comparative investigation on the effectiveness of polymerization method used for the preparation of PS was performed using Sty:EBiB of 500:1. The results suggested that ATRP was the least efficient method as shown through its slowest rate of polymerization and uncontrolled polymer characteristics (M_n and PDI). ARGET ATRP, on the other hand, gave the highest polymerization rate (M_n of 66.5 kDa was achieved in 24 h), although the obtained PDI of 1.54 suggested that the polymerization by ARGET ATRP was still not well controlled. Concurrent RAFT-ARGET ATRP, with polymerization under control of 2 equilibria (one for RAFT, the other for ARGET ATRP), provided a copolymer product with a better control over M_n and PDI. Thus, concurrent RAFT-ARGET ATRP was chosen as the method to be used for polymerization of high molecular weight PS and copolymers.

PS and PS-*co*-PMAPOSS were synthesized with target molecular weight higher than 100 kDa to ensure electrospinnability. When Sty:EBiB exceeded 500:1 (target M_n of 50 kDa), polymerization was not well controlled. Nevertheless, the molecular weight of the obtained copolymers closely resembled that of the target molecular weight of 130 kDa. The composition of MAPOSS in the copolymer calculated by both methods (from ^{1}H NMR and TGA data) progressively increased with the MAPOSS composition in the feed. The compositions calculated from ^{1}H NMR data seemed to be greater than the anticipated whereas the composition calculated from TGA data was underestimated when compared with the MAPOSS in the feed.

As for the block copolymer, early attempt to synthesize PS-*b*-PMAPOSS from PS macroinitiator by direct polymerization of MAPOSS was unsuccessful. This may be explained as a result of steric hindrance inherited with the bulky POSS group. In later attempt, Sty or methyl methacrylate (MMA) was mixed with MAPOSS in the syntheses of the second block in order to overcome the problem due to steric hindrance. An increase of %MAPOSS was noticeable whereas the molecular weight of the synthesized copolymer was still lower than expected.

PS and PS-*co*-PMAPOSS fiber mats were fabricated using electrospinning with THF and DMF as solvent. PS as-spun fiber mat were shown to be affected by various solvent ratios of THF and DMF, with THF resulted in beads with almost no fiber was obtained while DMF alone resulted in fiber with wider fiber diameter distribution as compared to the mixed solvent of THF and DMF. PS-*r*-PMAPOSS, however, behaved differently than homopolymer PS, with PS-*r*-PMAPOSS could only swell but not dissolve in DMF. With THF, obtained fiber had narrow fiber diameter distribution, smooth surface and was very dense. Addition of DMF in solvent, however, caused as-spun fibers to display various degrees of roughness and porosity and much wider fiber diameter distribution. In the case of block copolymer, as-spun fibers had very small fiber diameter but comparable roughness to random copolymer with higher %MAPOSS. PS-*b*-(PMMA-*r*-PMAPOSS), however, had very poor consistency in fiber diameter as compared with other block copolymers and surface roughness seemed to be random. Investigation by SEM/EDS technique showed that elemental composition of PS-*r*-PMAPOSS fiber surface changed according to solvent used, decreasing silicon content (MAPOSS moiety) on the surface was found with increasing DMF content. XRD spectra also showed that solvent affected phase morphology of PS-*r*-PMAPOSS This implied that the morphology of PS-*co*-PMAPOSS fiber was driven by DMF-induced phase separation.

Despite distinct morphology acquired, several improvements must be done before PS-*co*-PMAPOSS can be used in applications. First, porous morphology only occur in the presence of DMF in solvent, which also cause fiber diameter to be inconsistent. This requires further refining for better control of fiber diameter. Second, fiber diameter of the random copolymer are consistently large (2-7 μm)

which could be an obstacle for some practical usages that may require nanoscale morphology. Both of these issues might be resolved by reducing polymer molecular weight (similar to the case of block copolymer with lower molecular weight), reduce concentration of polymer solution used in electrospinning, albeit at the risk of bead formation, and/or increase polarity of polymer solution through addition of salt. Finally, due to chemical inertness of PS, further modification to chemical functionality of fiber is difficult. This requires either drastic method, such as plasma treatment to introduce polar functional groups, or incorporation of another compound into fibers.

REFERENCES

[1]   Li, G., Wang, L., Ni, H., and Pittman, C.U. Jr. Polyhedral oligomeric silsesquioxane (POSS) polymers and copolymers: a review. J. Inorg. Organomet. P. 11 (2001) : 123-154.

[2]   Zhang, W., and others. Effect of methyl methacrylate/polyhedral oligomeric silsesquioxane random copolymers in compatibilization of polystyrene and poly(methyl methacrylate) blends. Macromolecules 35 (2002) : 8029-8038.

[3]   Joshi, M., Butola, B. S., Simon, G., and Kukaleva, N. Rheological and viscoelastic behavior of HDPE/octamethyl-POSS nanocomposites. Macromolecules 39 (2006) : 1839-1849.

[4]   Kim, C.K., Kim, B.S., Sheikh, F.A., Lee, U.S., Khil, M. S., and Kim, H.Y. Amphiphilic poly(vinyl alcohol) hybrids and electrospun nanofibers incorporating polyhedral oligosilsesquioxane. Macromolecules 40 (2007) : 4823-4828.

[5]   Xue, Y., and others. Superhydrophobic electrospun POSS-PMMA copolymer fibres with highly ordered nanofibrillar and surface structures. Chem. Commun. (2009) : 6418-6420.

[6]   Cozza, E.S., Monticelli, O., and Marsano, E. Electrospinning: a novel method to incorporate POSS into a polymer matrix. Macromol. Mater. Eng. 295 (2010) : 791–795.

[7]   Zhang, W., Fang, B., Walther, A., and Müller, A.H.E. Synthesis via RAFT polymerization of tadpole-Shaped organic/inorganic hybrid poly(acrylic acid) containing polyhedral oligomeric silsesquioxane (POSS) and their self-assembly in water. Macromolecules 42 (2009) : 2563-2569.

[8]   Gu, X., Wu, J., and Mather, P.T. Polyhedral oligomeric silsesquioxane (POSS) suppresses enzymatic degradation of PCL-based polyurethanes. Biomacromolecules 12 (2011) : 3066–3077.

[9]   Li, D. and Xia, Y. Electrospinning of nanofibers: Reinventing the wheel? Adv. Mater. 16 (2004) : 1151-1170.

[10]   Tsai, P.P., Schreuder-Gibson, H., and Gibson, P. Different electrostatic method for making electricity magnet filters. J. Electrostatics. 54 (2002) : 333-341.

[11]   Hafemann, B., and others. Use of collagen/elastin-membrane for the tissue engineering of dermis. Burns 25 (1999) : 373-384.

[12]   Im, J.S., Kim, J.G., Lee, S.H., and Lee, Y.S. Effective electromagnetic interference shielding by electrospun carbon involving $Fe_2O_3/BaTiO_3/MWCNT$ additives. Mater. Chem. Phys. 124 (2010) : 434-438.

[13]   Gibson, P.W., Schreuder-Gibson, H.L., and Rivin, D. Electrospun fiber mats: Transport properties. American Institute of Chemical Engineers 45 (1999) : 90-195.

[14]   Gouma, P.I. Nanostructured polymorphic oxides for advanced chemo-sensors. Rev. Adv. Mater. Sci. 5 (2003) : 147-154.

[15]   Tuteja, A., and others. Designing superoleophobic surfaces. Science 318 (2007) : 1618-1622.

[16]   Bellis, M. Invention of polystyrene and styrofoam. About.com [Online]. 2009. Available from : http://inventors.about.com/od/pstartinventions/ a/styrofoam.htm [2012, April 23].

[17]   Jarusuwannapoom, T., and others. Effect of solvents on electro-spinnability of polystyrene solutions and morphological appearance of resulting electrospun polystyrene fibers. Eur. Polym. J. 41 (2005) : 409–421.

[18]   Baker, S.C., and others. Characterisation of electrospun polystyrene scaffolds for three-dimensional in vitro biological studies. Biomaterials 27 (2006) : 3136–3146.

[19]   Zhu, Y., Zhang, J., Zheng, Y., Huang, Z., Feng, L., and Jiang, L. Stable, superhydrophobic, and conductive polyaniline/polystyrene films for corrosive environments. Adv. Funct. Mater. 16 (2006) : 568–574.

[20]   Wang, N., Zhao, Y., and Jiang, L. Low-cost, thermoresponsive wettability of surfaces: poly(*N*-isopropylacrylamide)/polystyrene composite films prepared by electrospinning. Macromol. Rapid Commun. 29 (2008) : 485–489.

[21]   Kailas, L., Nysten, B., and Bertrand, P. Difference in the annealing behaviour of thin films of PS/PMMA blends and copolymers as revealed by ToF-SIMS and AFM. Surf. Interface Anal. 36 (2004) : 1227–1230.

[22]   Wei, M., Kang, B., Sung, C., and Mead, J. Core-sheath structure in electrospun nanofibers from polymer blends. Macromol. Mater. Eng. 291 (2006) : 1307–1314.

[23]   Hirai, T., Leolukman, M., Hayakawa, T., Kakimoto, M., and Gopalan, P. Hierarchical nanostructures of organosilicate nanosheets within self-organized block copolymer films. Macromolecules 41 (2008) : 4558-4560.

[24]   Otsu, T., Yoshida, M., and Tazaki, T. A model for living radical polymerization. Makromol. Chem., Rapid Commun. 3 (1982) : 133 – 140.

[25]   Wang, J., and Matyjaszewski, K. Controlled "living" radical polymerization. atom transfer radical polymerization in the presence of transition-metal complexes. J. Am. Chem. Soc. 117 (1995) : 5614-5615.

[26]   Jakubowski, W., Min, K., and K., Matyjaszewski, K. Activators regenerated by electron transfer for atom transfer radical polymerization of styrene. Macromolecules 39 (2006) : 39-45.

[27]   Chiefari, J., and others. Living free-radical polymerization by reversible addition-fragmentation chain transfer: The RAFT process. Macromolecules 31 (1998) : 5559-5562.

[28]   Nicolaÿ, R., Kwak, Y., and Matyjaszewski, K. A green route to well-defined high-molecular-weight (co)polymers using ARGET ATRP with alkyl pseudohalides and copper catalysis. Angew. Chem. 122 (2010) : 551 – 554.

[29]   Kwak, Y., Nicolaÿ, R., and Matyjaszewski, K. Concurrent ATRP/RAFT of styrene and methyl methacrylate with dithioesters catalyzed by copper(I) complexes. <u>Macromolecules</u> 41 (2008) : 6602-6604.

[30]   Magenau, A. J. D., Kwak, Y., and Matyjaszewski, K. ATRP of methacrylates utilizing CuIIX$_2$/L and copper wire. <u>Macromolecules</u> 43 (2010) : 9682–9689.

[31]   Ishihara, N., Seimiya, T., Kuramoto, M., and Uoi, M. Crystalline syndiotactic polystyrene. <u>Macromolecules</u> 19 (1986) : 2464–2465.

Appendix

Molecular Weight and Molecular Weight Distribution of Polymers

Different average molecular weight value can be defined through different statistical methods. Two methods are chosen for determination of polymer molecular weight:

(1) Number Average Molecular Weight

Number Average Molecular Weight (M_n) is an arithmathic mean where all data point (in this case, molecular weight of each polymer chain) weights equally.The equation for calculation of M_n is as followed:

$$M_n = \frac{\Sigma N_i M_i}{\Sigma N_i}$$

(A-1)

Where N_i is a number of polymer chains with molecular weight = M_i.

(2) Weight Average Molecular Weight

Weight Average Molecular Weight (M_w) is a weight mean where all data point (in this case, molecular weight of each polymer chain) weight differently, with weight of each molecular weight depends on weight it contributes. The equation for calculation of M_w is as followed:

$$M_w = \frac{\Sigma W_i M_i}{\Sigma W_i}$$

(A-2)

Where W_i is a weight of polymer chains with molecular weight = M_i.

For GPC, calibration curve must be created using polymer standard with narrow molecular weight. Elution volume or elution time (x axis) are plotted against logarithm of molecular weight of polymer standards (y axis). From the calibration curve, relationship between elution volume or elution time and molecular weight can be described using the following polynomial equation:

$$\log M = A_0 + A_1 V + A_2 V^2 + ... + A_n V^n$$

(A-3)

Where M is molecular weight and V is corresponding elution volume (substitute with t for elution time). For an unknown sample, the intensity of signal at i^{th} data point correspond to weight-fraction (W_i) of polymer at molecular weight = M_i. Since weight-fraction can be derived from number and molecular weight of polymer chains:

$$W_i = N_i M_i$$

(A-4)

M_n can be described as followed:

$$M_n = \frac{\Sigma W_i}{\Sigma (W_i/M_i)}$$

(A-5)

Polydispersity Index

Polydispersity Index (PDI) is a measurement of polymer molecular weight distribution. PDI can be calculated from the following equation.

$$PDI = \frac{M_w}{M_n}$$

(A-6)

Since the way of the calculation make M_w always equal to or more than M_n, PDI value is always 1 or higher. For polymer with uniform chain length, PDI value approaches 1.

VITAE

Mr. Thanarath Pisuchpen was born on October 15th, 1986 in Bangkok, Thailand. He received the Degree of Bachelor of Science (Chemistry), Faculty of Science, Chulalongkorn University, Pathumwan, Bangkok, Thailland in 2009. In the same year, He was admitted to a Master's Degree in Program of Chemistry, Faculty of Science, Chulalongkorn University and completed the program in 2012. His address is 460 Thanon Nakhon Chai Sri, Dusit, Bangkok 10300.

Presentation in Conference

Oral Presentation   Thanarath Pisuchpen, Narupol Intasanta, Voravee P. Hoven "Synthesis and Electrospinning of Polyhedral Oligomeric Silsesquioxane-containing Copolymer" *2nd Polymer Conference of Thailand*, Convention Center, Chulabhorn Research Institute, Bangkok, October 20-21, **2011**

Poster   Thanarath Pisuchpen, Narupol Intasanta, Voravee P. Hoven "Polyhedral Oligomeric Silsesquioxane-Containing copolymers: Synthesis and Electrospinning" *The 6th Pure and Applied Chemistry International Conference (PACCON) 2012*, The Empress Hotel, Chiang Mai, January 11-13, **2012**